

# Tilted Dirac Fermions

## *Topological metals from band inversion*

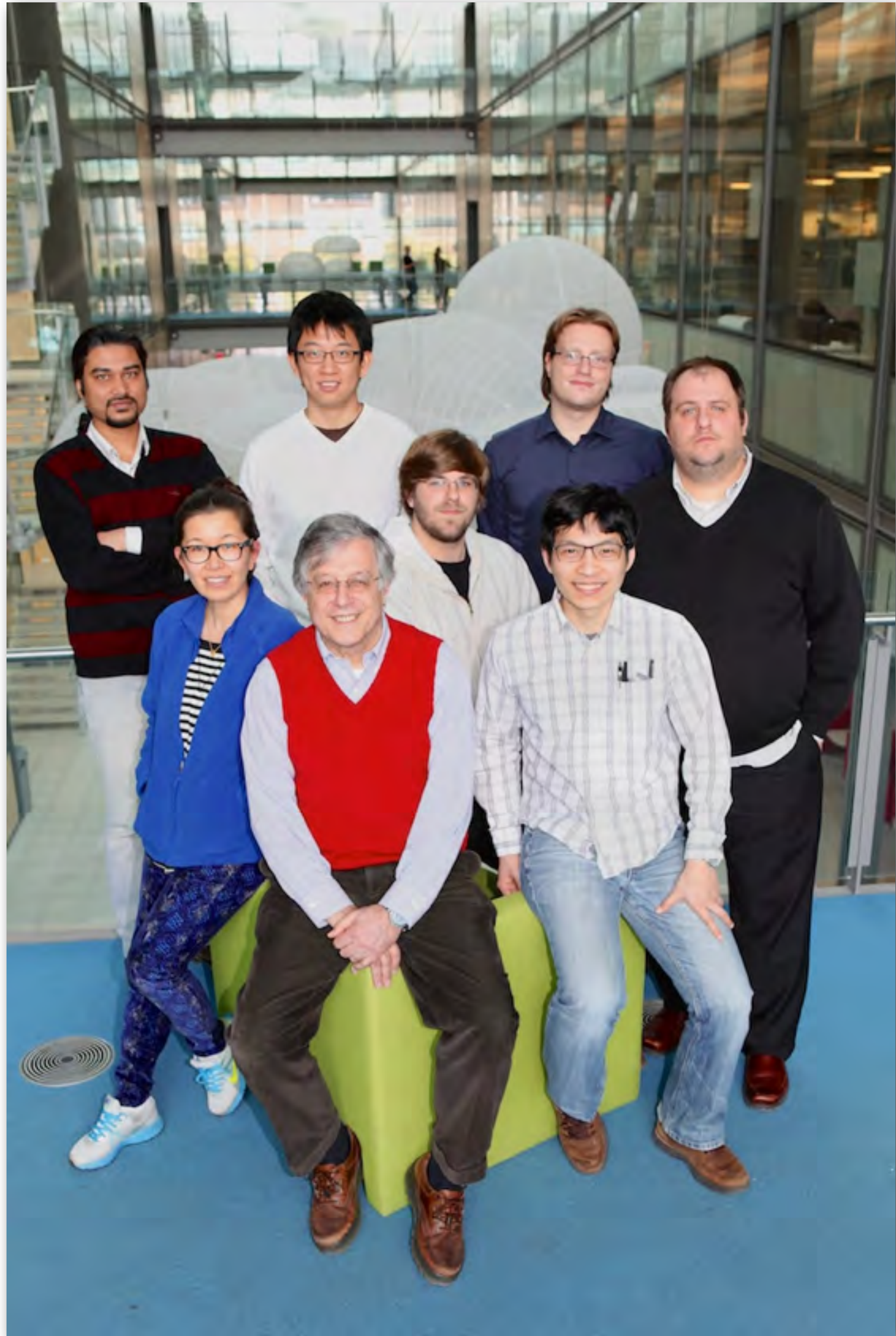
Lukas Muechler, Aris Alexandradinata, Titus Neupert and  
Roberto Car

Princeton University



ArXiv: 1604.01398

# Acknowledgements



Aris Alexandradinata

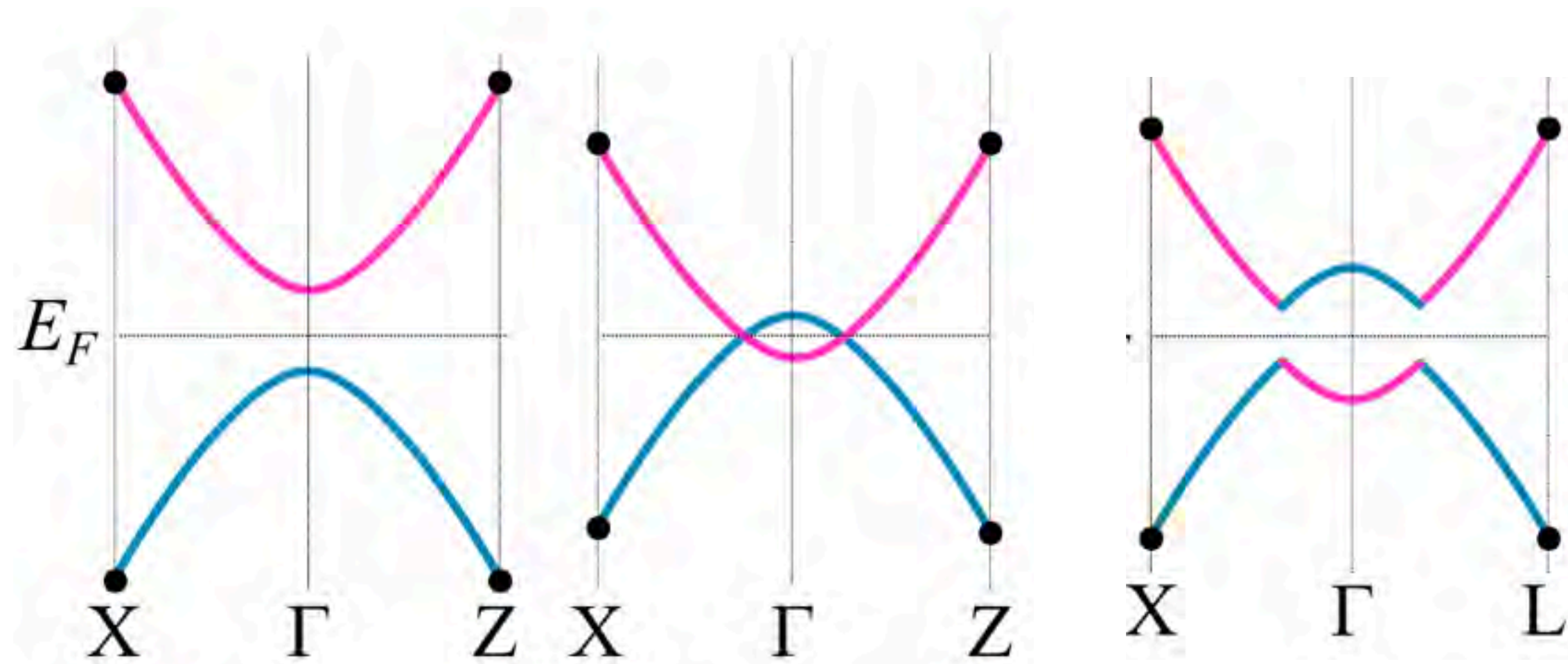


Roberto Car

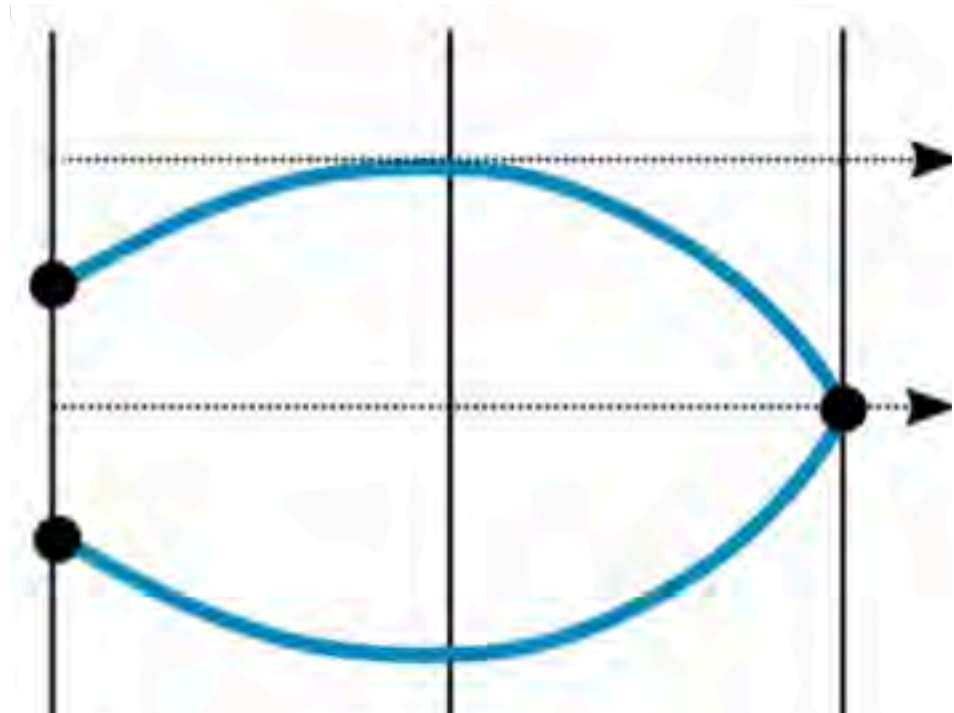


Titus Neupert

# Noninteracting SPTs



Topological (crystalline) Insulators

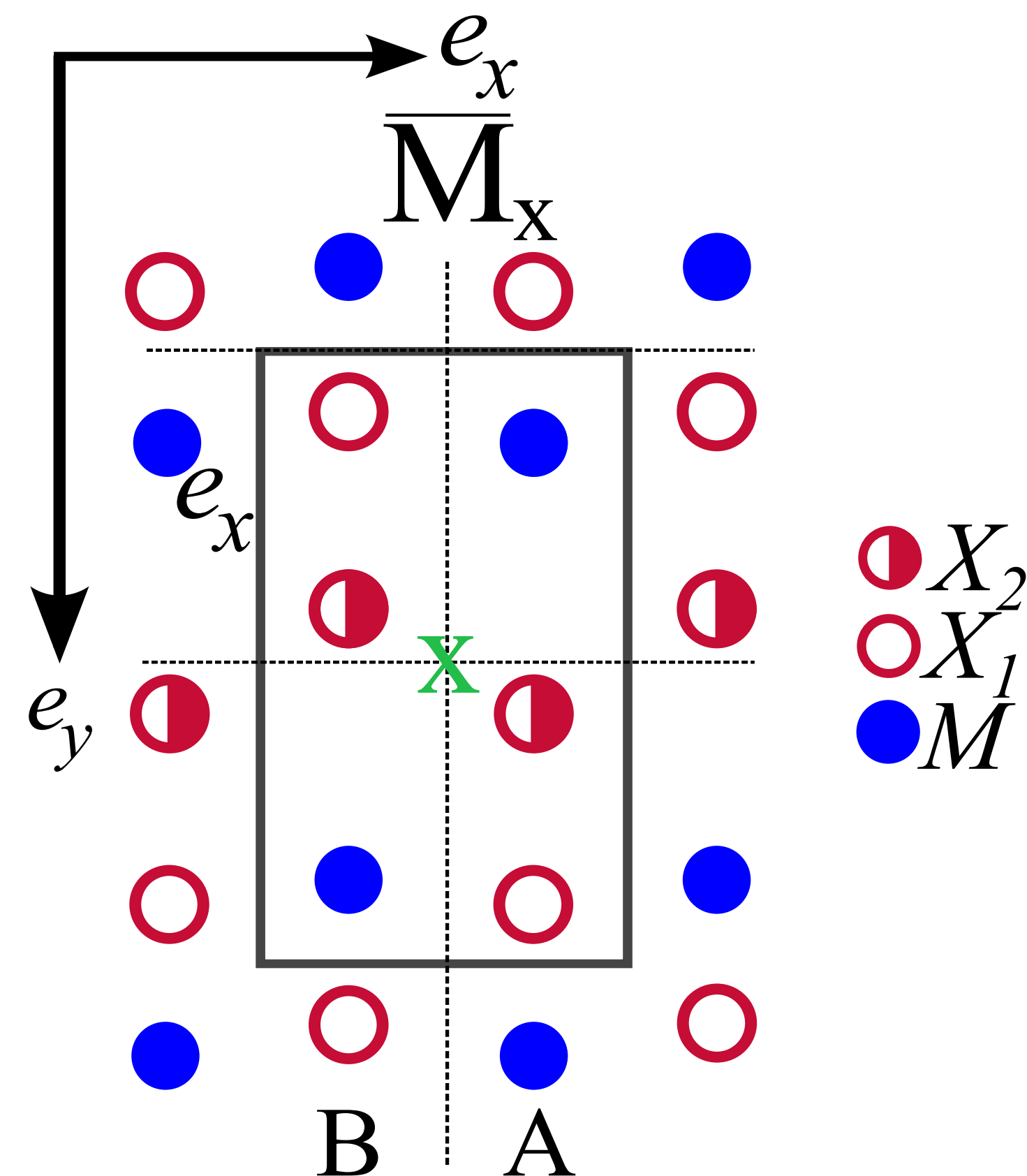


Gaplessness guaranteed by nonsymmorphic symmetries at certain electron fillings

# Non-symmorphic symmetries

Two types of symmetries

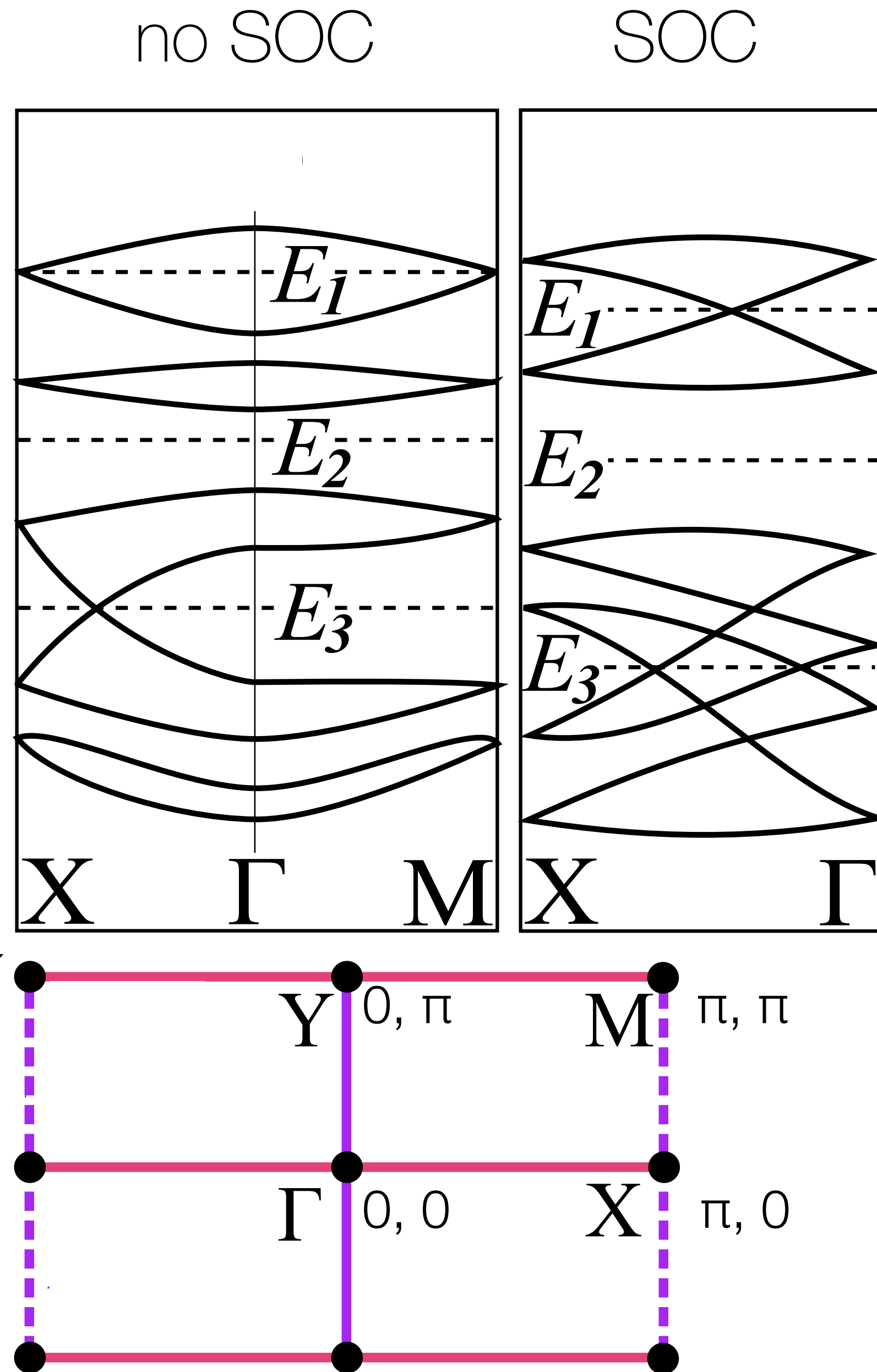
- ▶ symmorphic symmetries preserve origin
- ▶ non-symmorphic symmetries unavoidably translate spatial origin
- ▶ Examples:  $\text{MX}_2$  monolayers ( $\text{ZrI}_2, \text{MoTe}_2, \text{WTe}_2$ )
- ▶ Three symmetries: Screw rotation, Glide-reflection and inversion symmetry



# Band structures

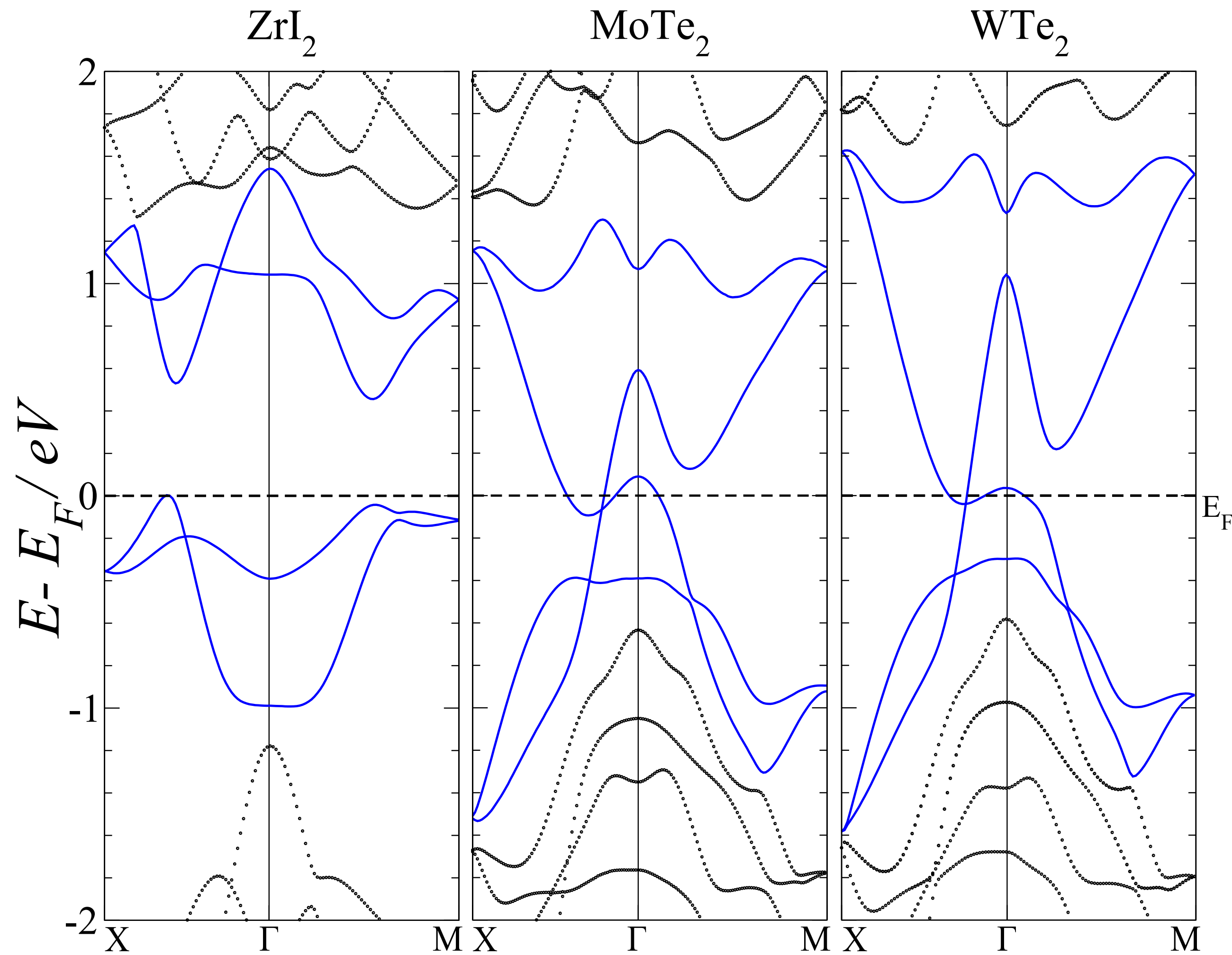
Three different types of band structures

- ▶ Filling enforced semimetal ( $E_1$ )
- ▶ Band insulators ( $E_2$ )
- ▶ topological semimetal due to band inversion ( $E_3$ )



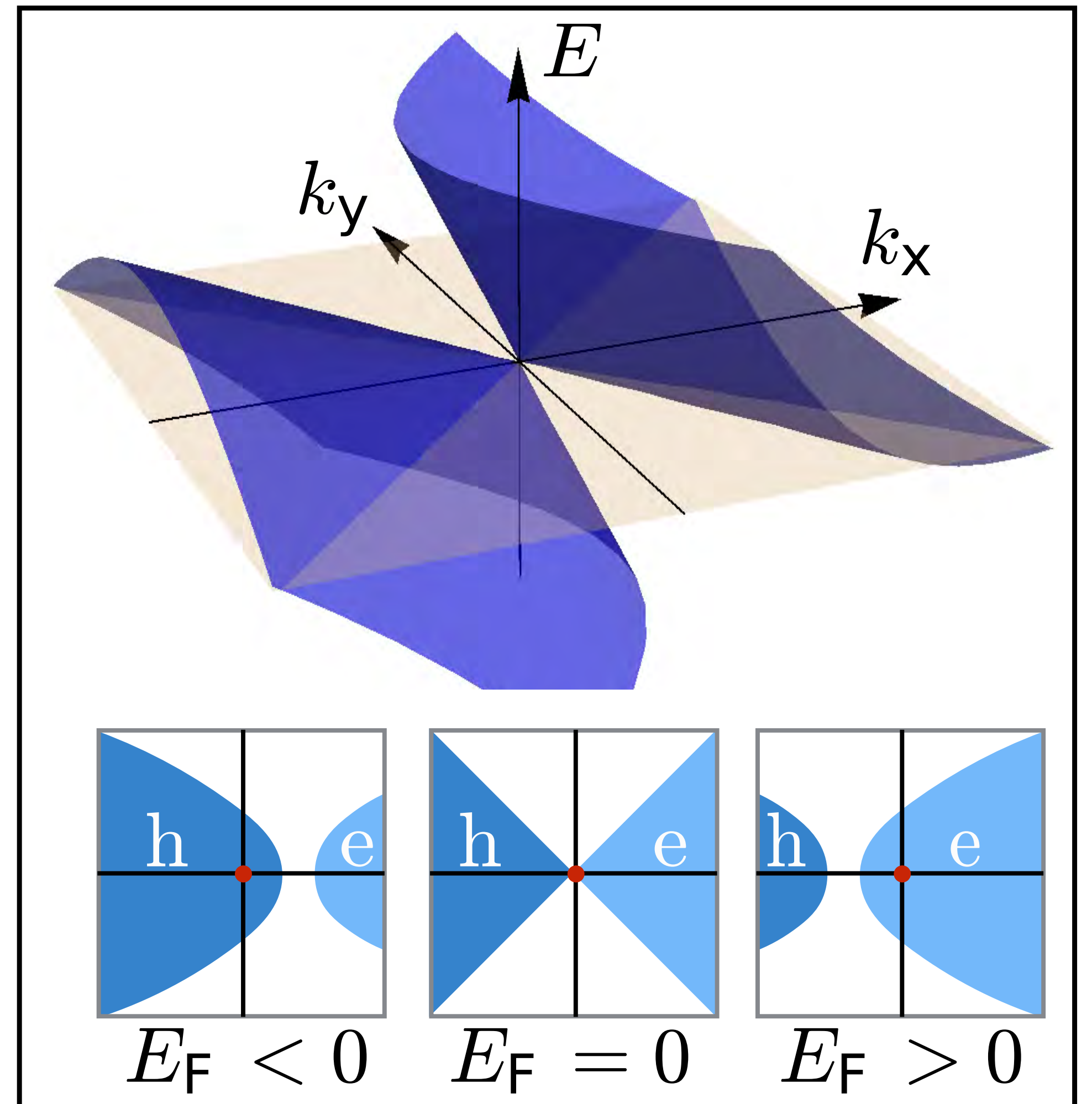
# Material examples

- ▶ New class of band-inverted topological semimetals
- ▶ Band inversion of orthogonal screw representations leads to robust Dirac crossing along  $\Gamma X$
- ▶ Type-II Dirac cones



# Type-II Dirac fermions

- ▶ Dirac cone tilts over to produce electron- and hole-like Fermi surfaces
- ▶ Only Fermi-surfaces that encircle the Dirac node carry Berry phase of  $\pi$



$$\mathcal{H}_{\text{II}}(\mathbf{k}) = u_x k_x \sigma_0 + v_x k_x \sigma_1 + v_y k_y \sigma_2$$

# Topological classification

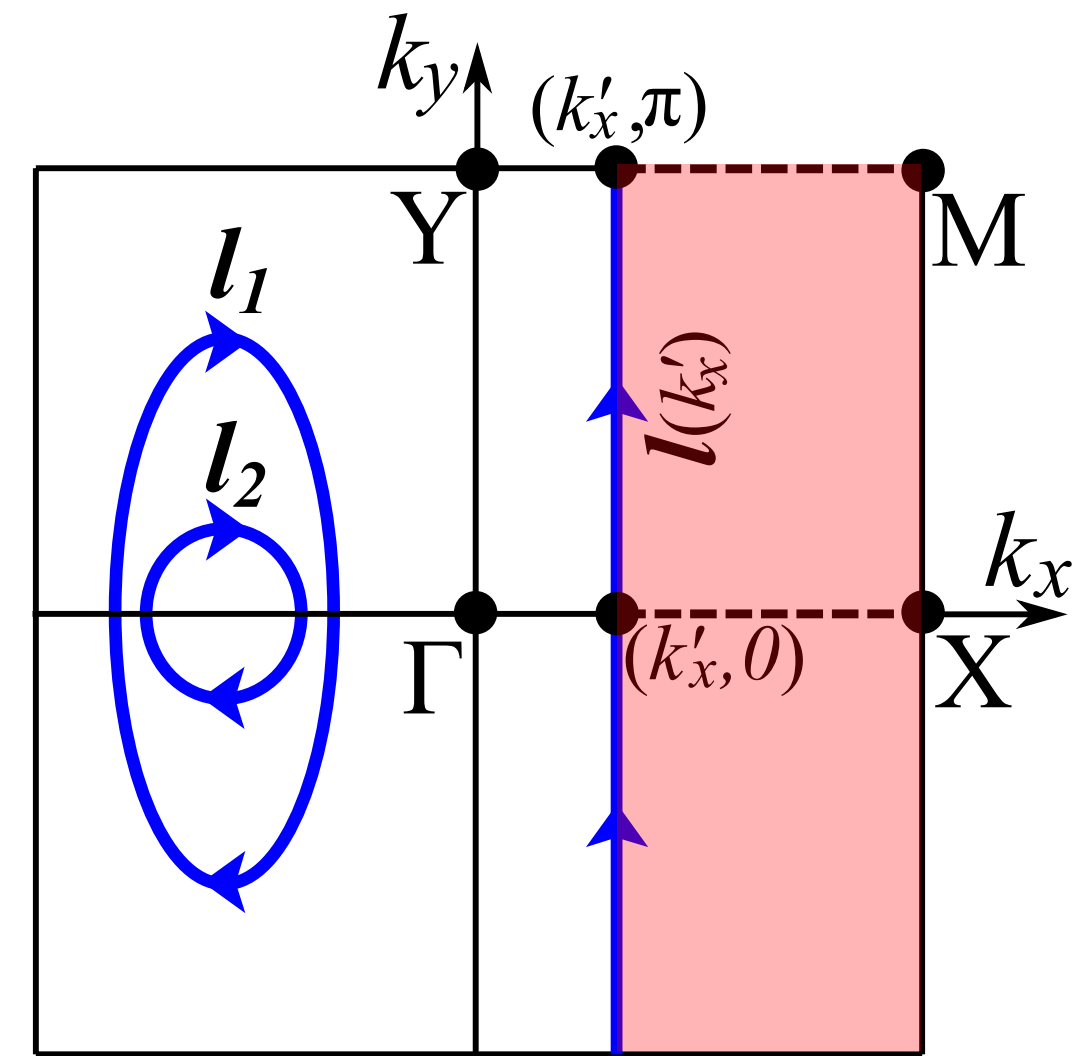
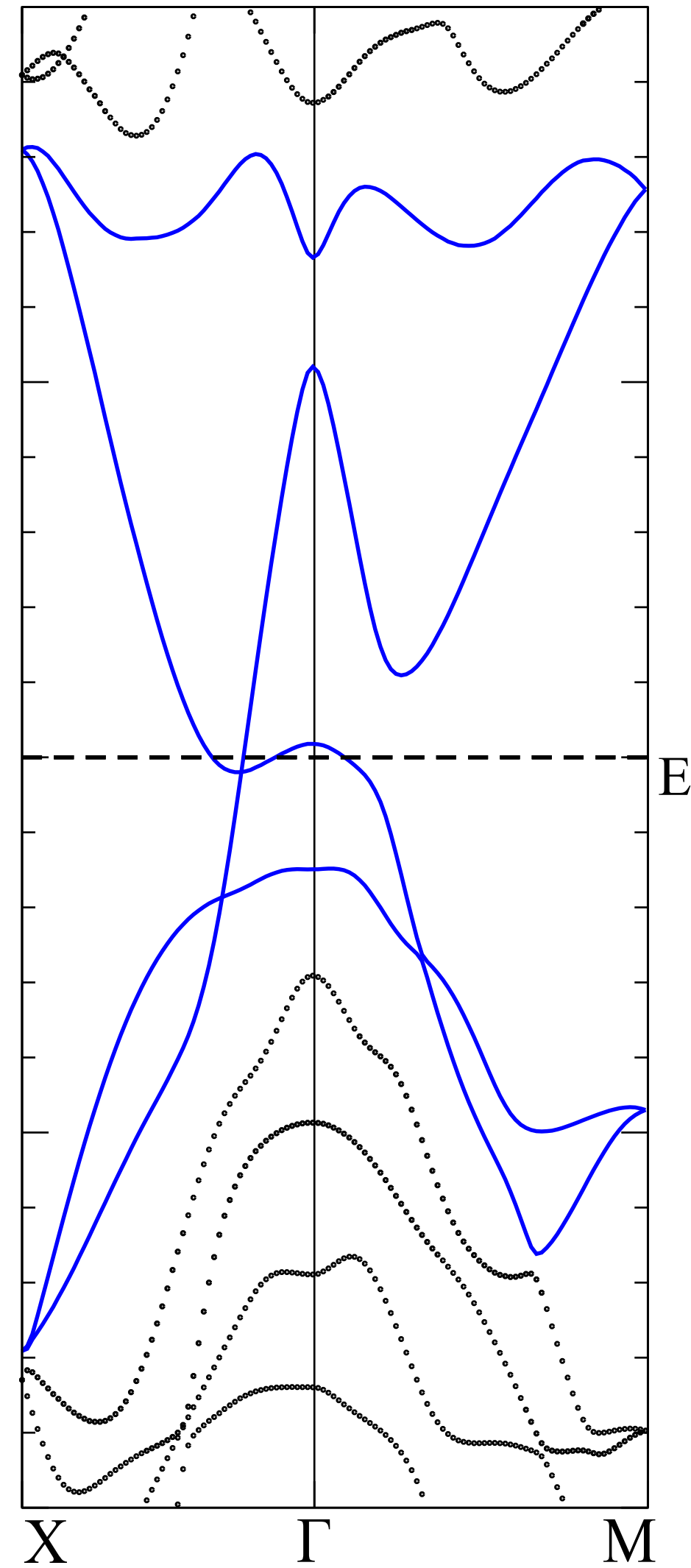
$$\mathcal{W}[l] = \overline{\exp} \left[ - \int_l d\mathbf{k} \cdot \mathbf{A}(\mathbf{k}) \right]$$

$$\mathbf{A}(\mathbf{k})_{ij} = \langle u_{i,\mathbf{k}} | \nabla_{\mathbf{k}} u_{j,\mathbf{k}} \rangle$$

$$e^{i\Phi_{U(1)}[l]} \equiv \exp \left[ - \int_l d\mathbf{k} \cdot \text{Tr}[\mathbf{A}(\mathbf{k})] \right] = \det[\mathcal{W}[l]]$$

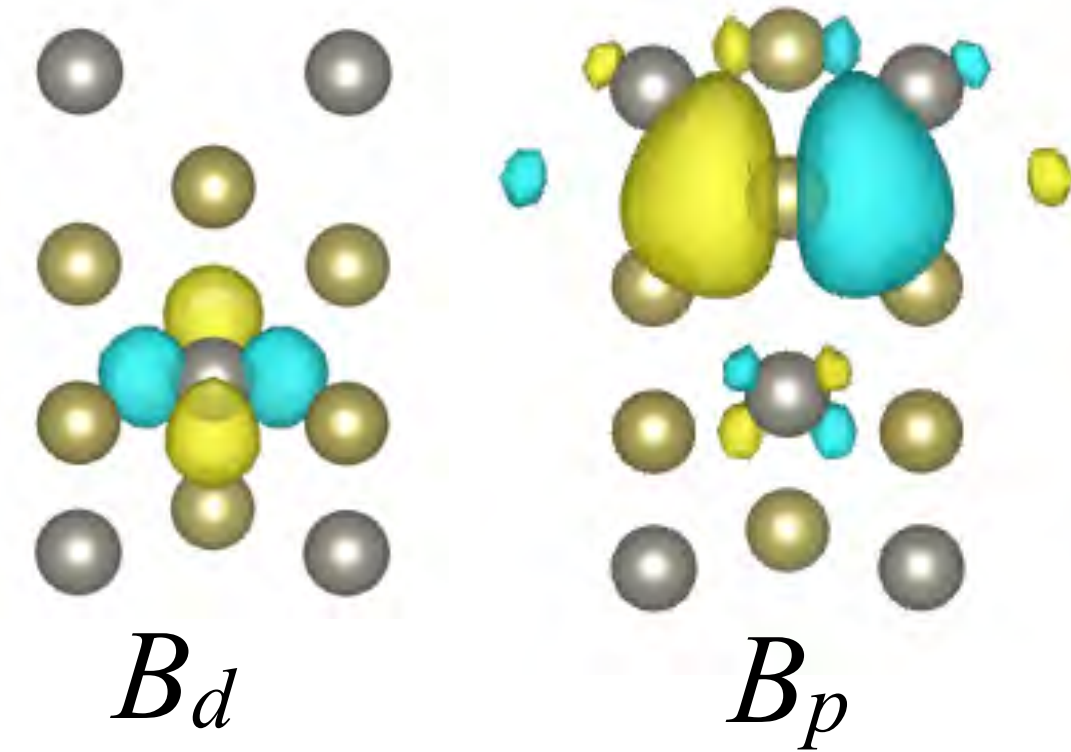
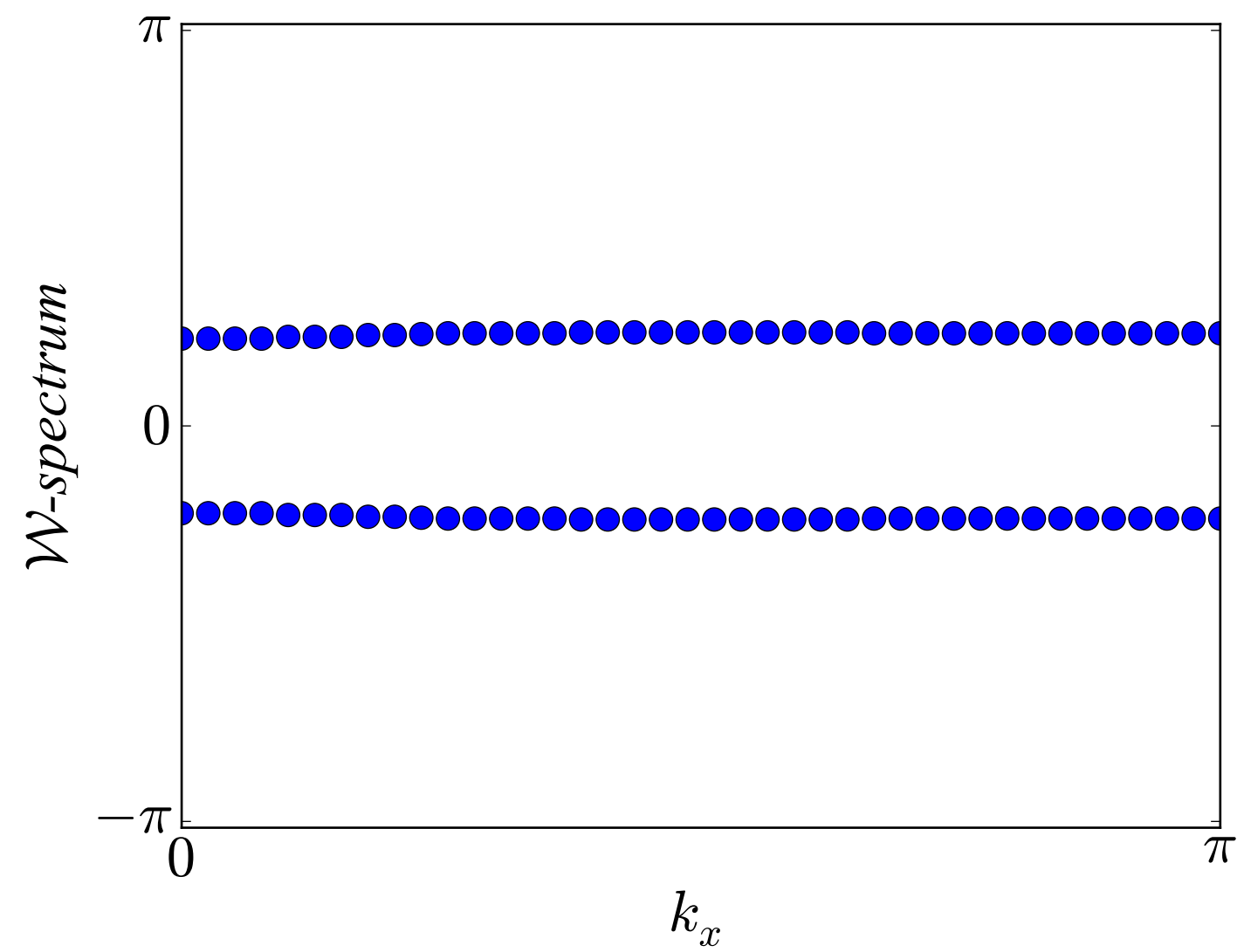
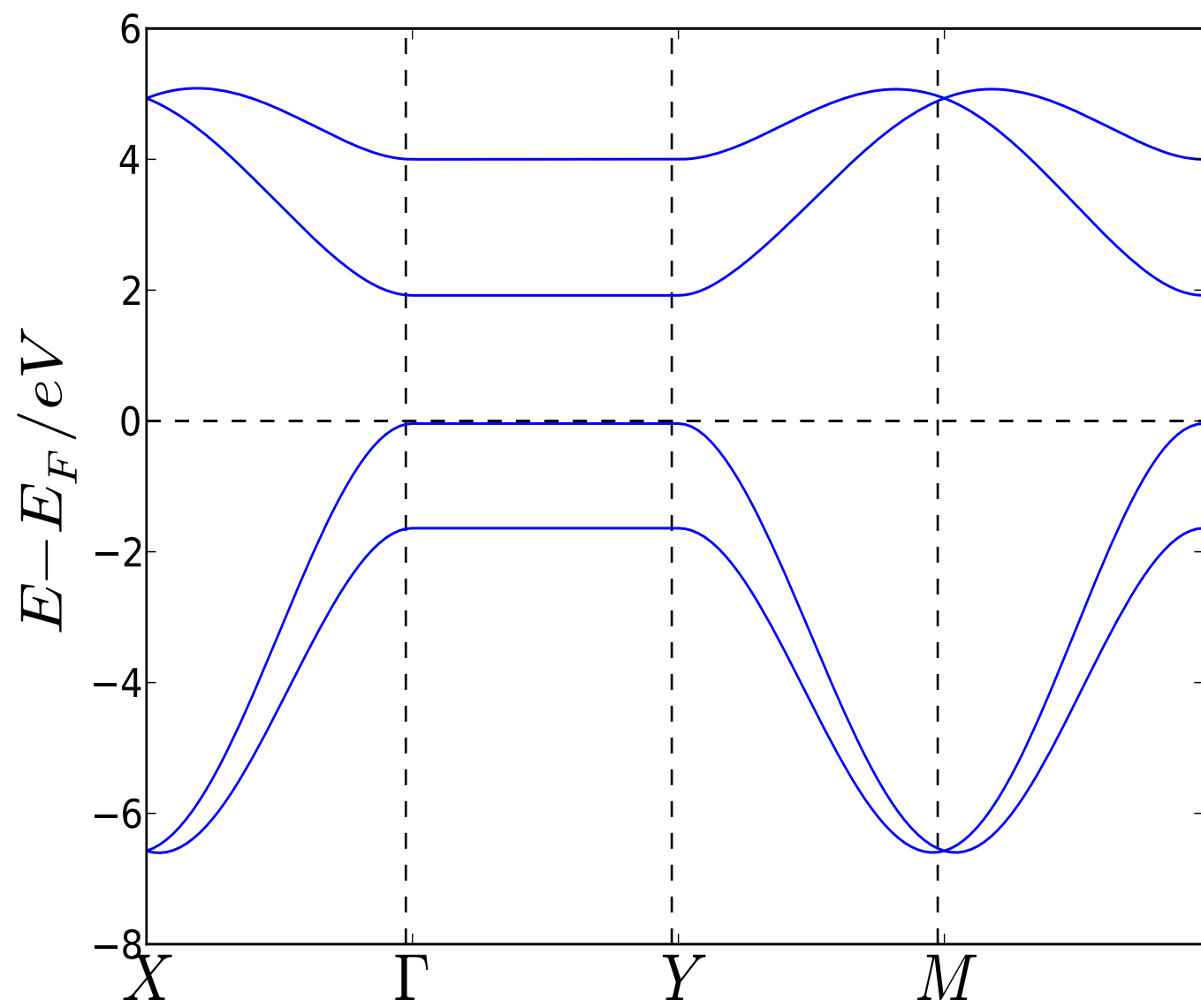
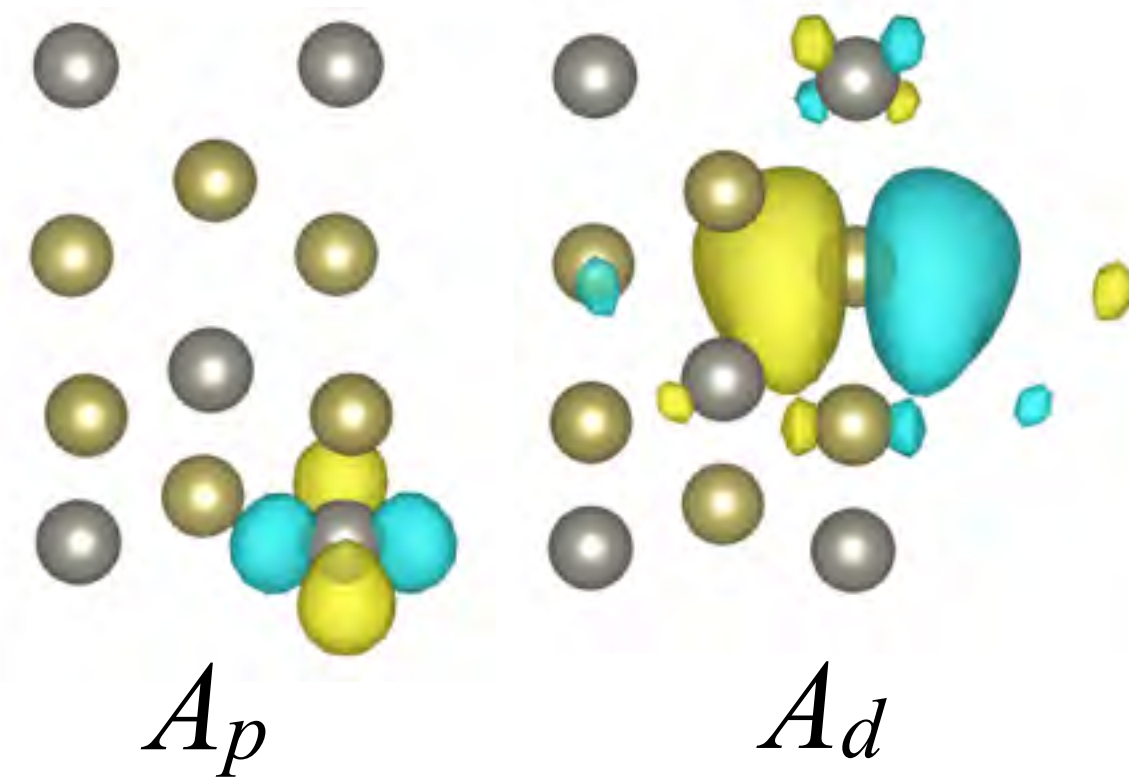
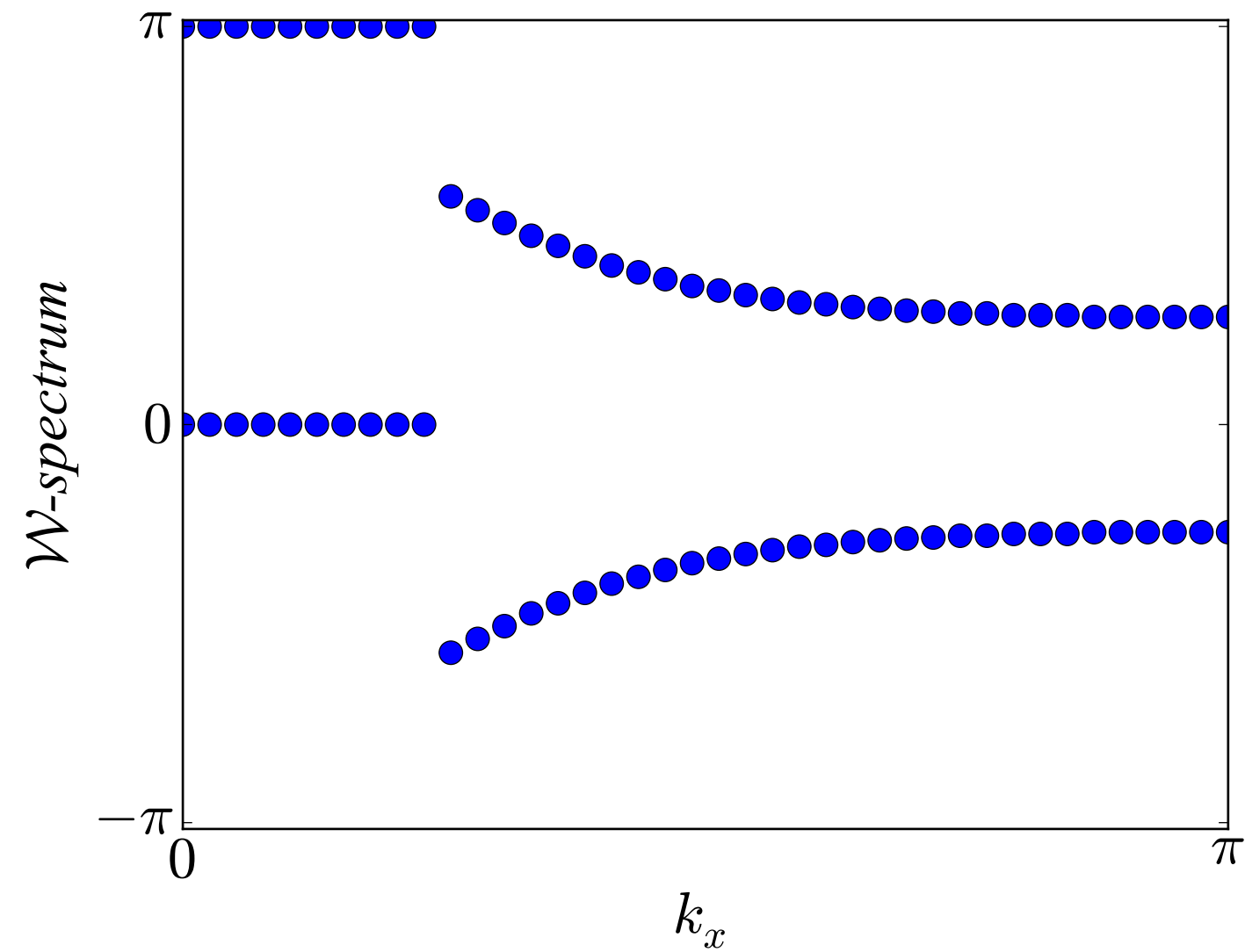
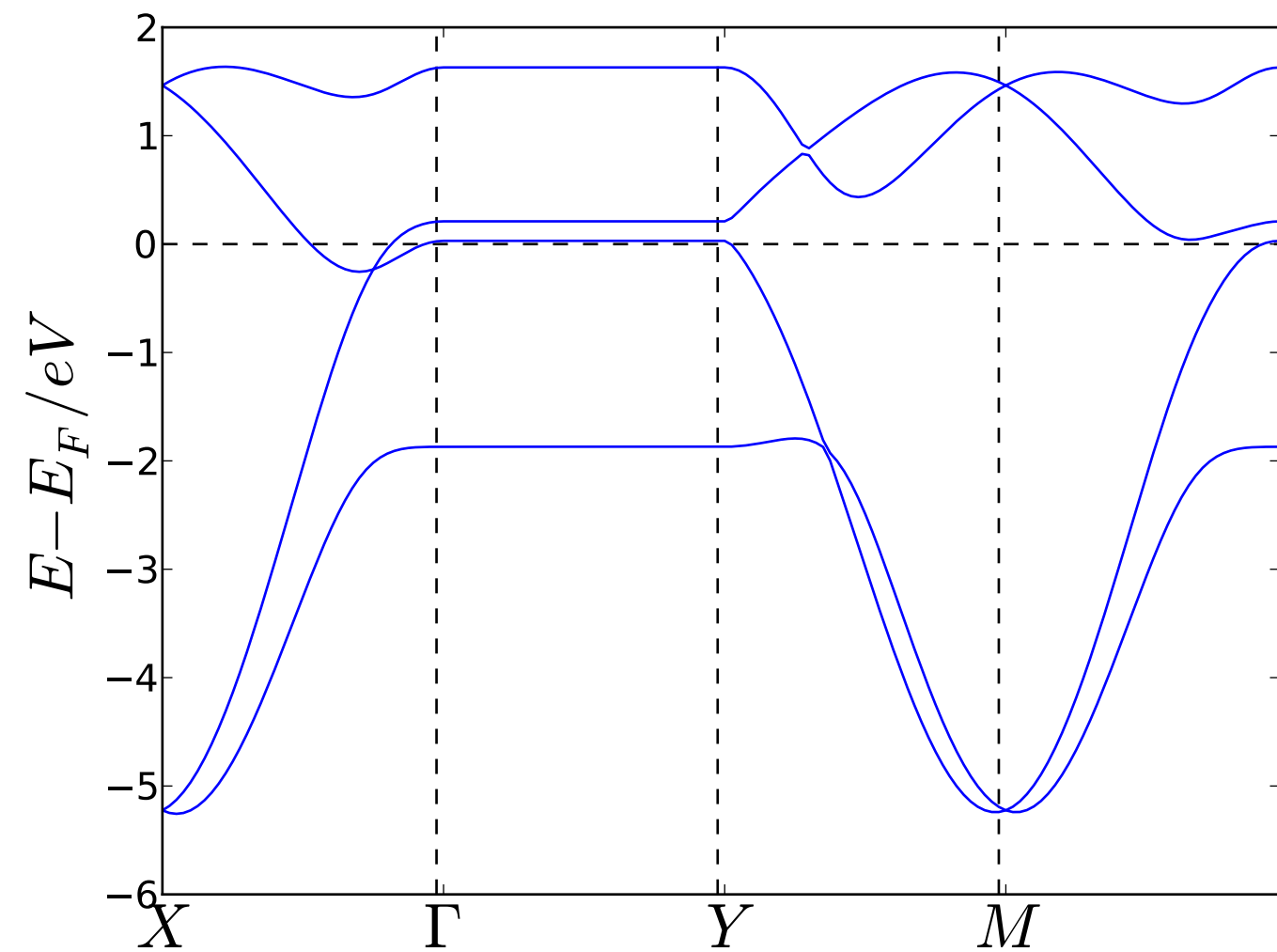
| $N_{+,\mathbf{k}_1}$ | $N_{-,\mathbf{k}_2}$ | $\mathcal{W}(k_x)$        | $\bar{D}_{l(k_x)}$ | $D_{\mathbf{k}_1} - D_{\mathbf{k}_2} \text{ mod } 2$ |
|----------------------|----------------------|---------------------------|--------------------|--|
| 1                    | 1                    | $[\lambda_1 \lambda_1^*]$ | 0                  | 0  |
| 2                    | 1                    | $[+-]$                    | 1                  | 1  |
| 2                    | 0                    | $[- -]$                   | 2                  | 0  |
| 2                    | 2                    | $[++]$                    | 2                  | 0  |

WTe<sub>2</sub>





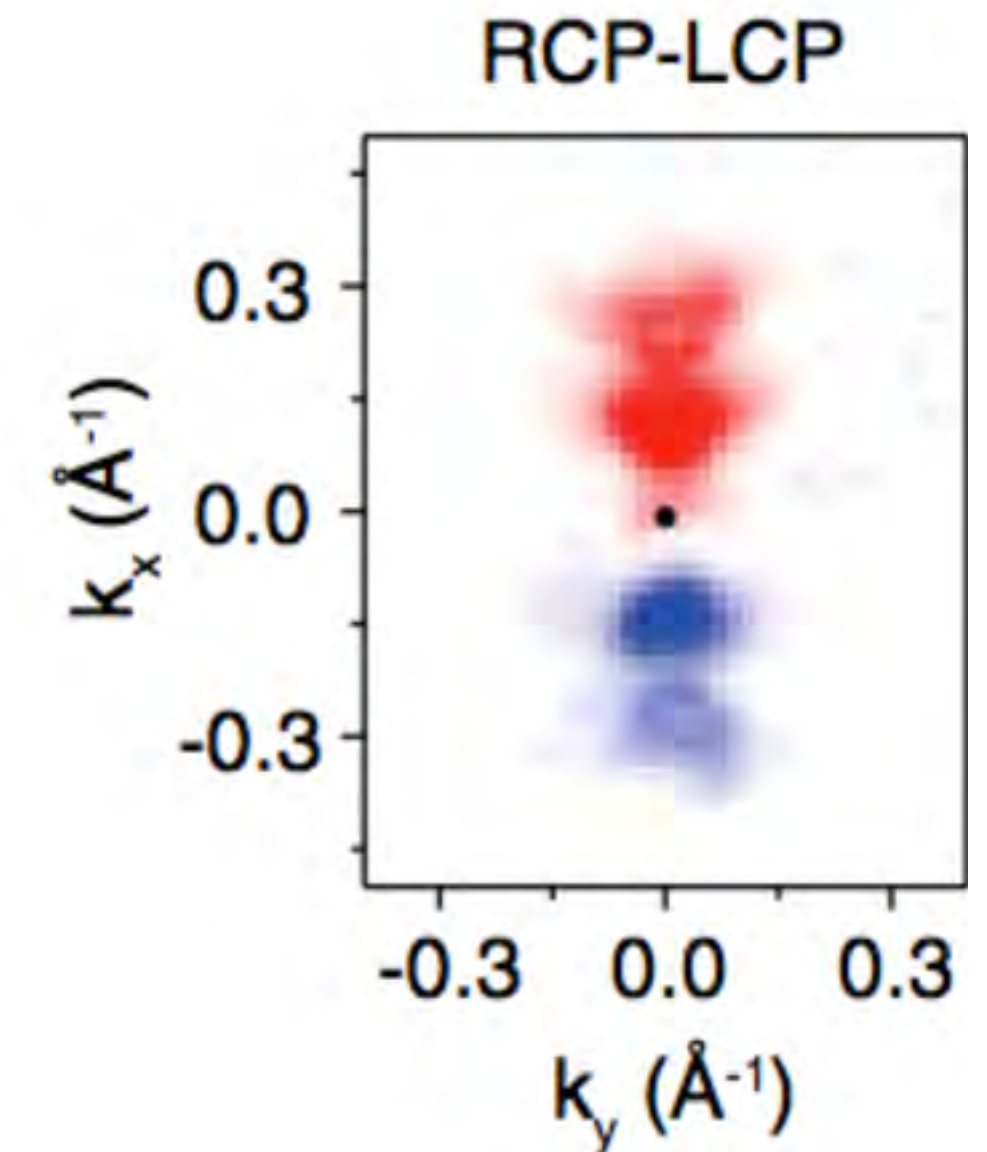
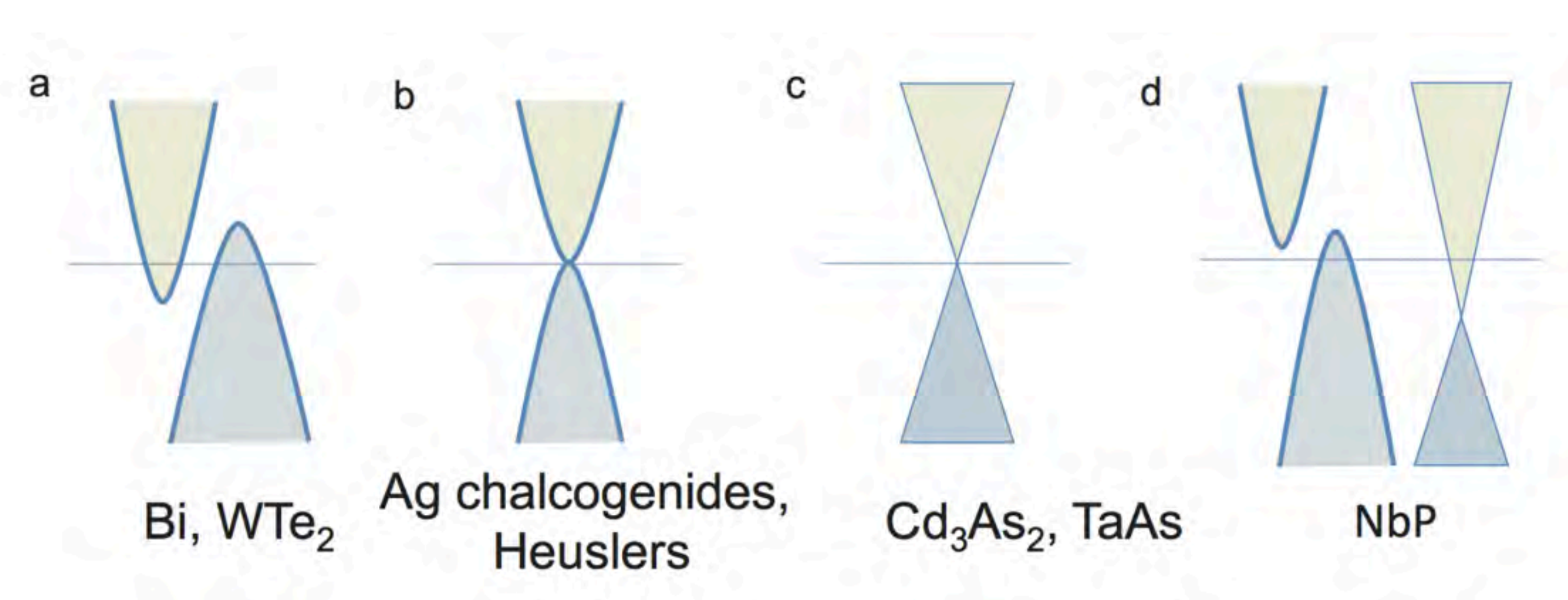
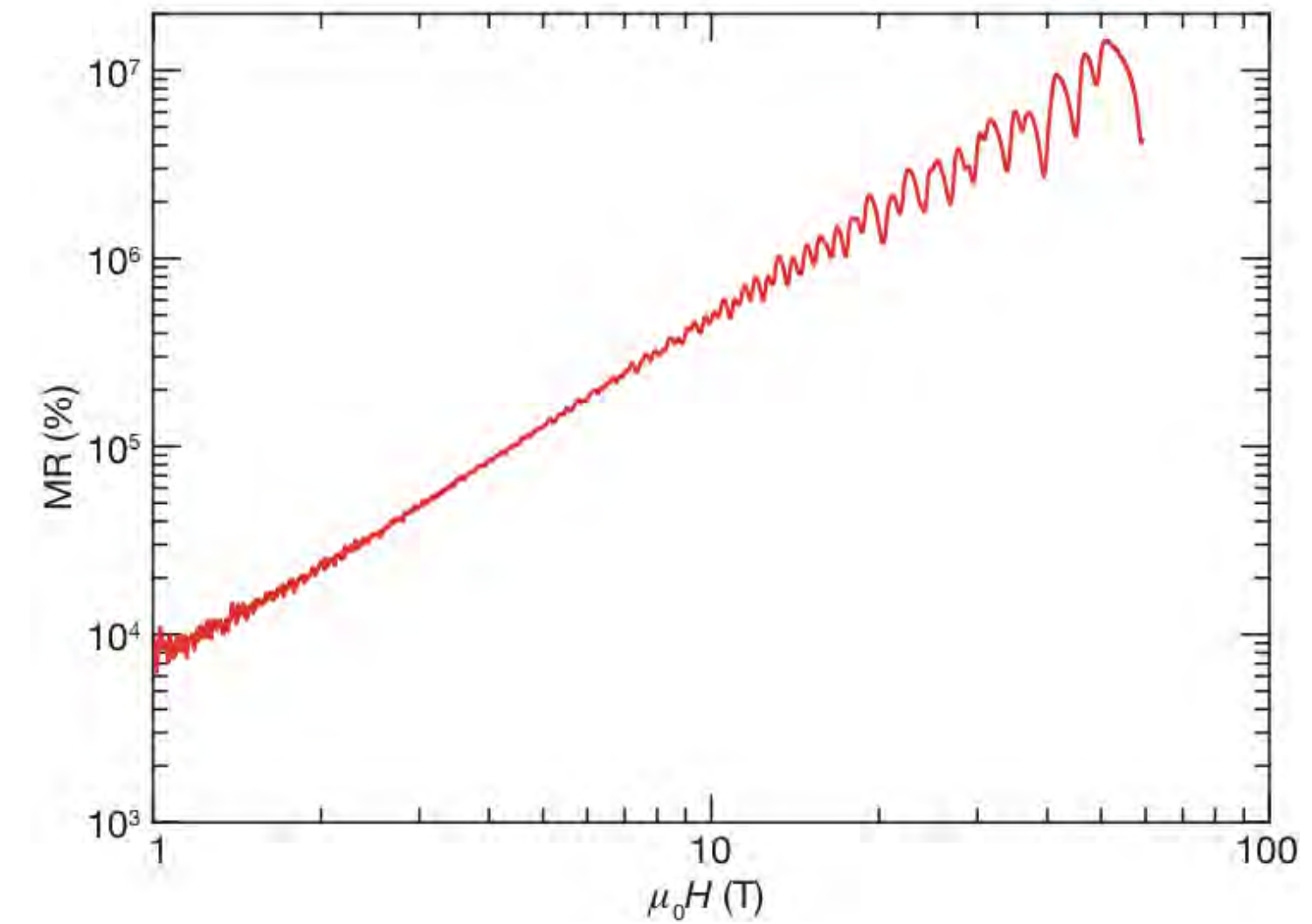
*Tight-binding model:  $WTe_2$*



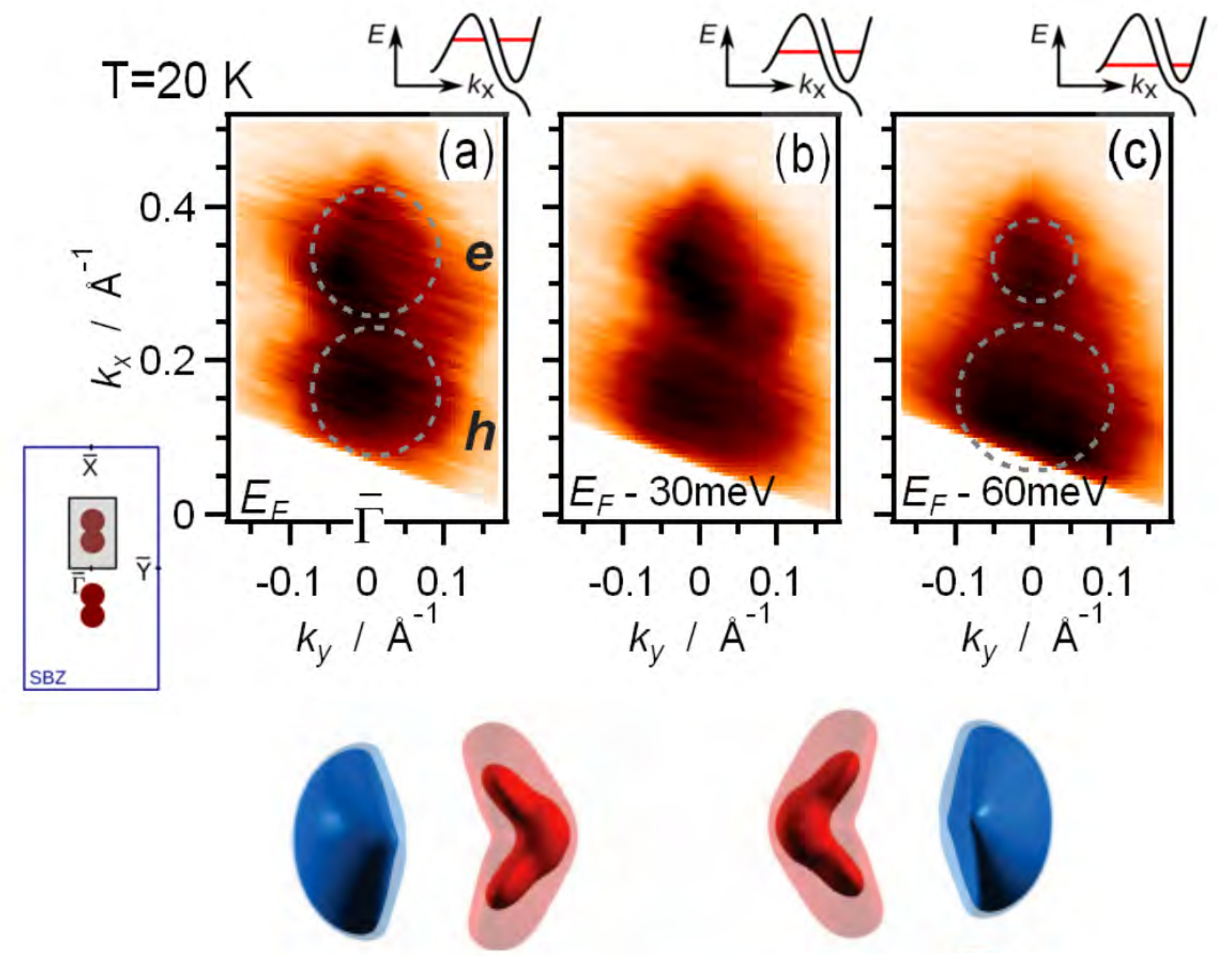
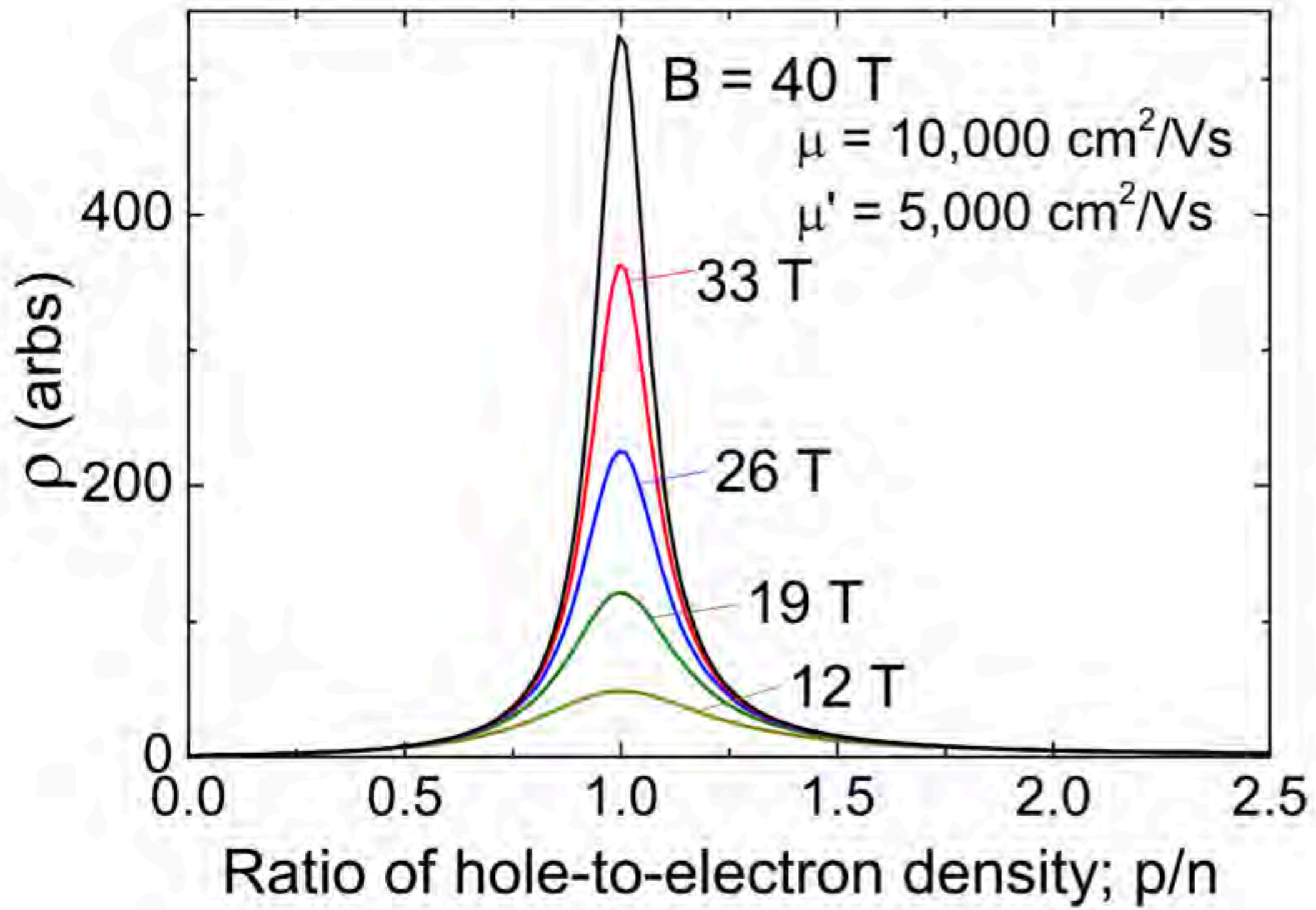
# Consequences for 3D material

WTe<sub>2</sub>: ludicrous magnetoresistance

- ▶  $1.7 \times 10^6$  % at 2K and 9T
- ▶ Mobilities up to 167 000 cm<sup>2</sup>/Vs
- ▶ (compensated) electron and hole pockets
- ▶ Circular Dichroism in ARPES experiments

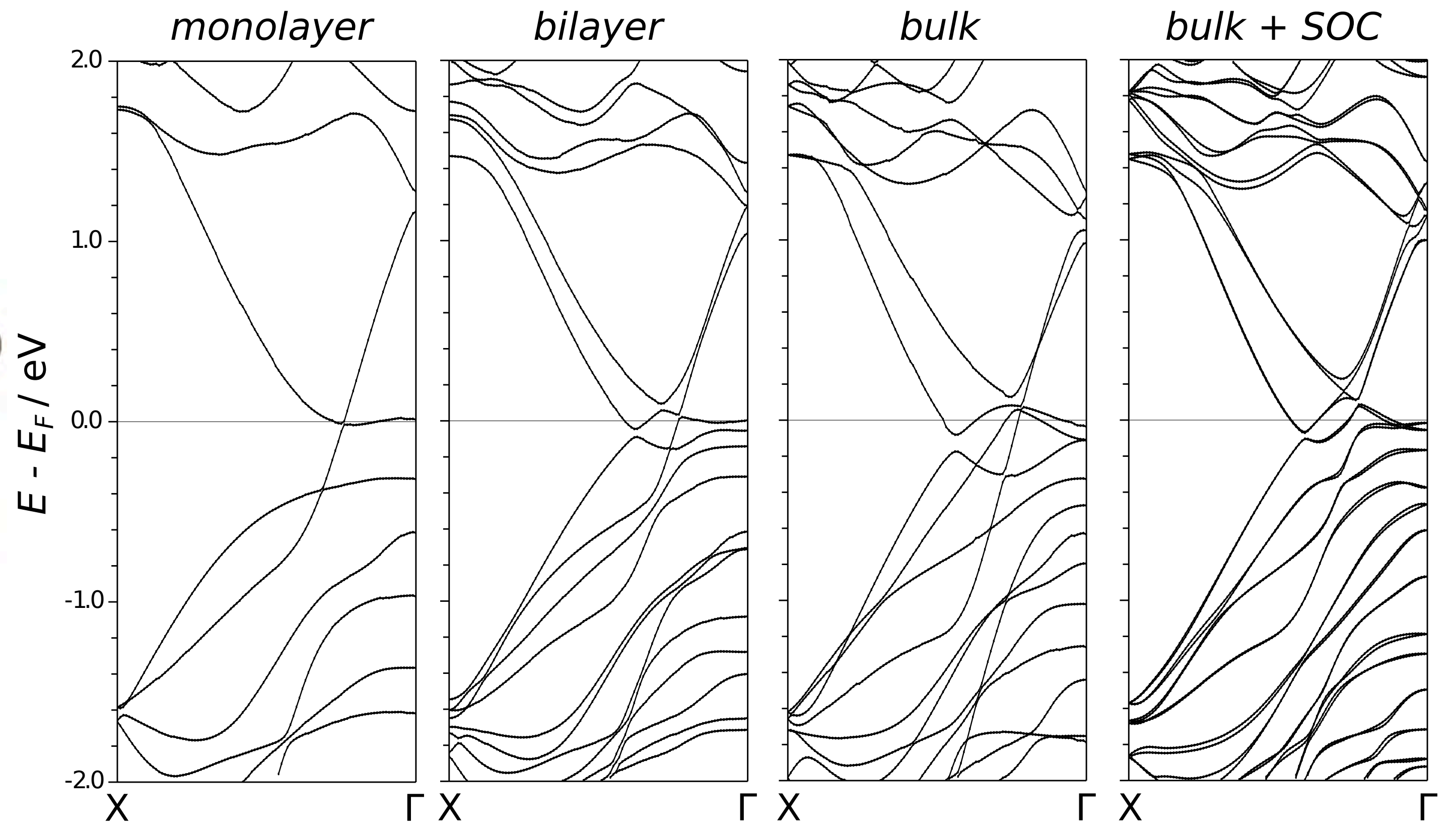
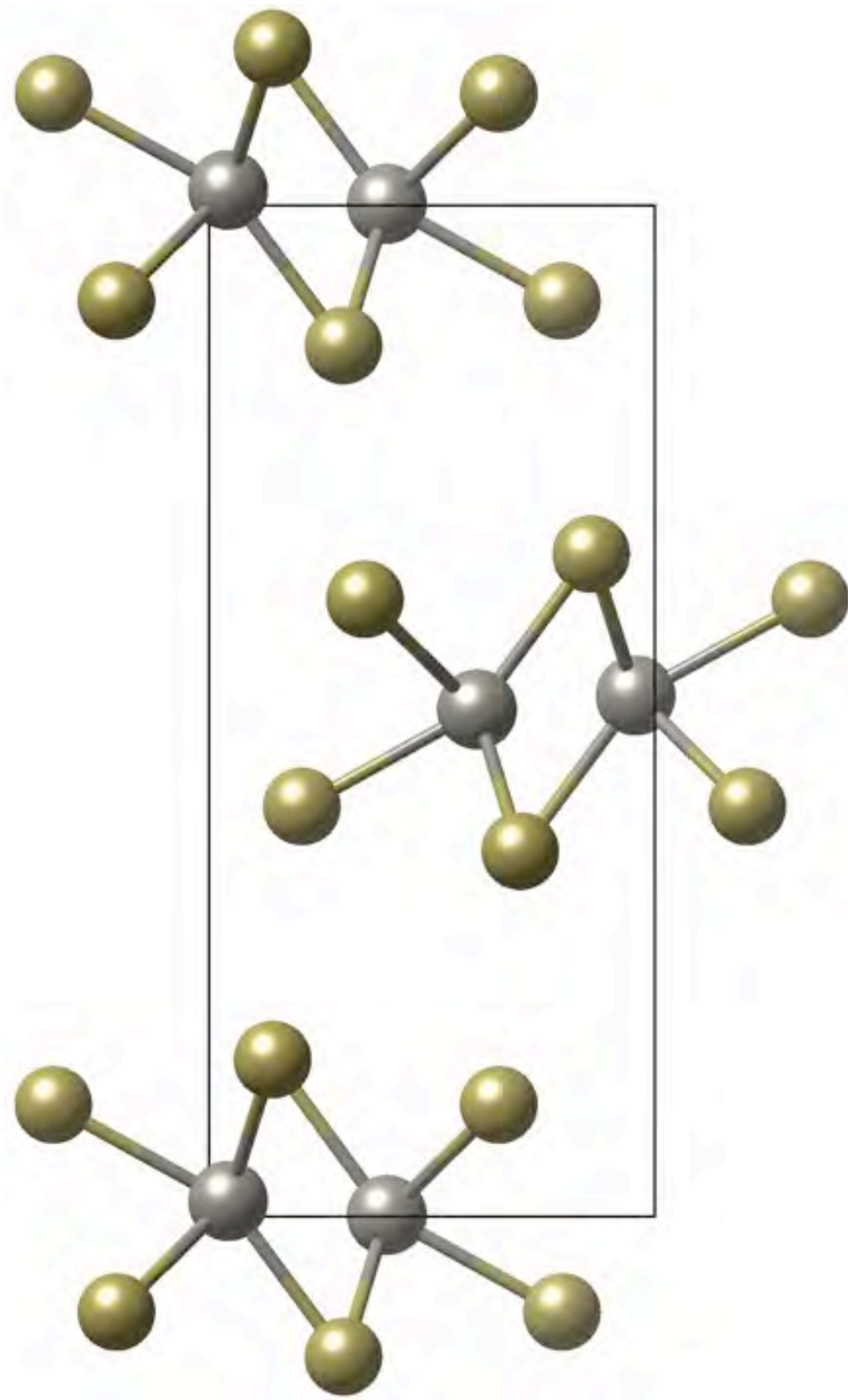


# High-MR theory

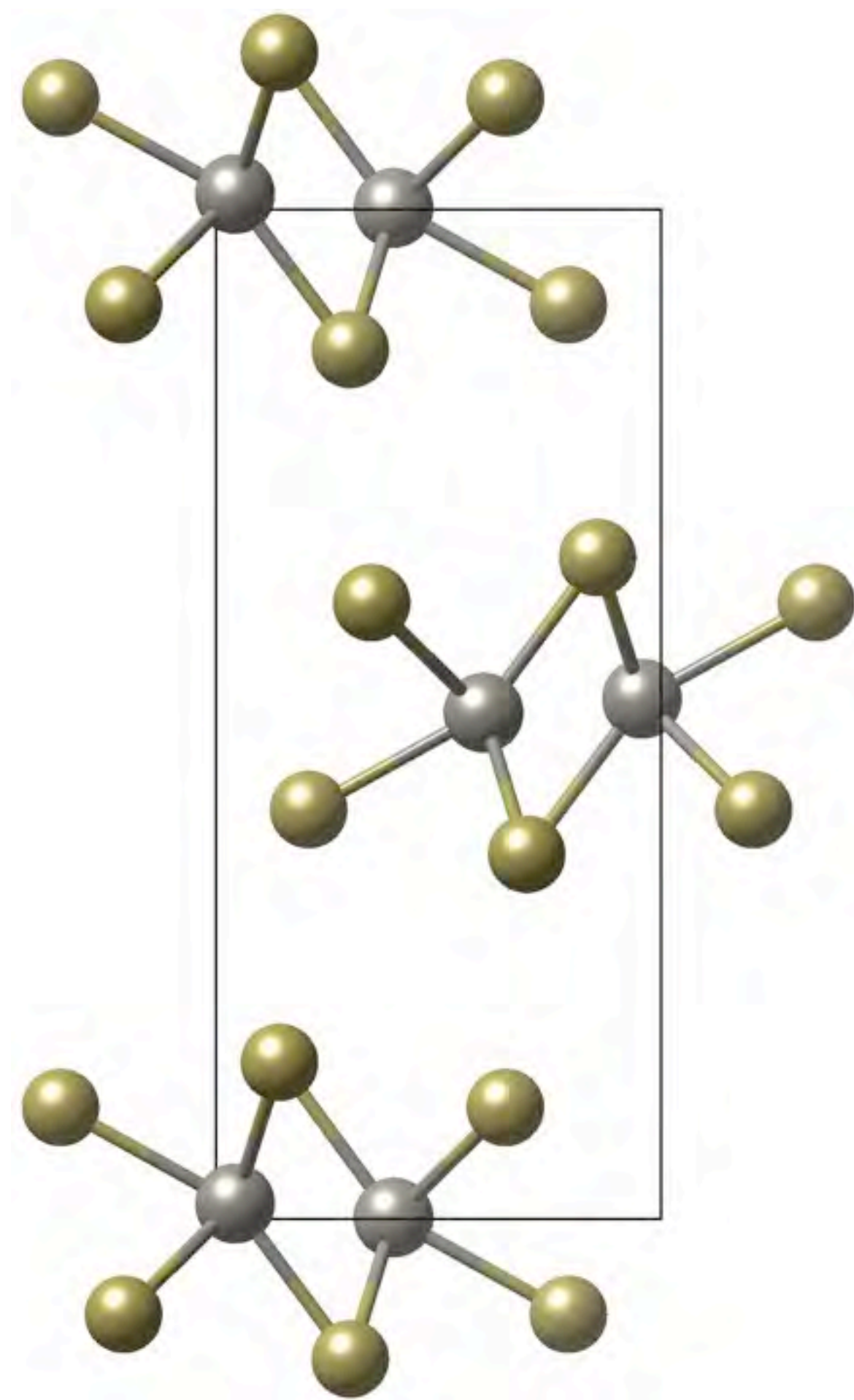


$$[\rho(H) - \rho(0)] / \rho(0) = \mu_e \mu_h B^2$$

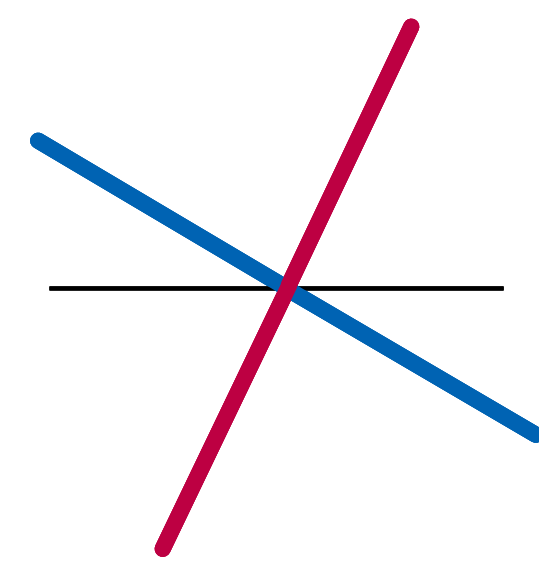
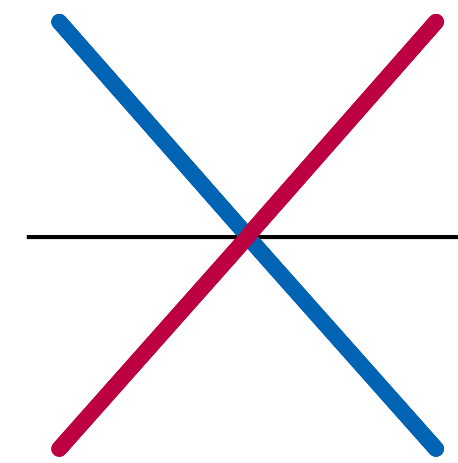
*WTe<sub>2</sub> / MoTe<sub>2</sub>*



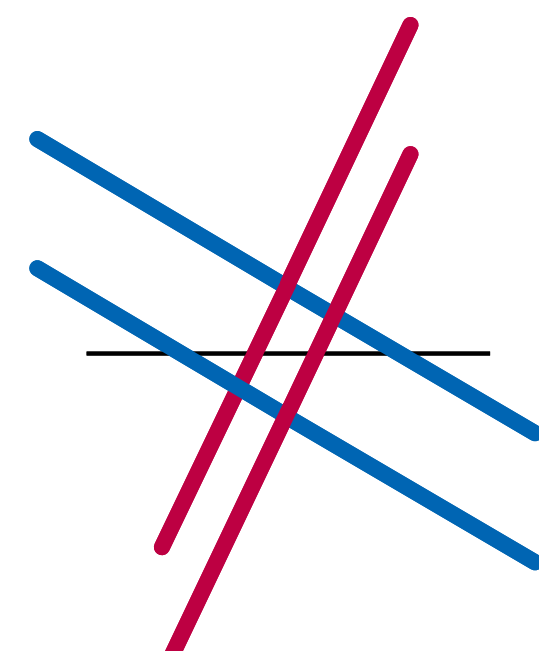
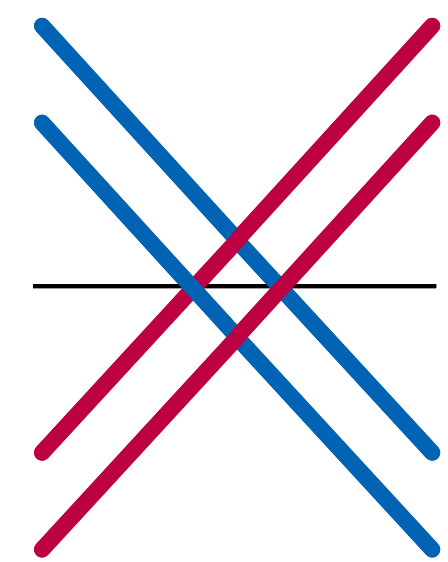
# Electron and hole pockets



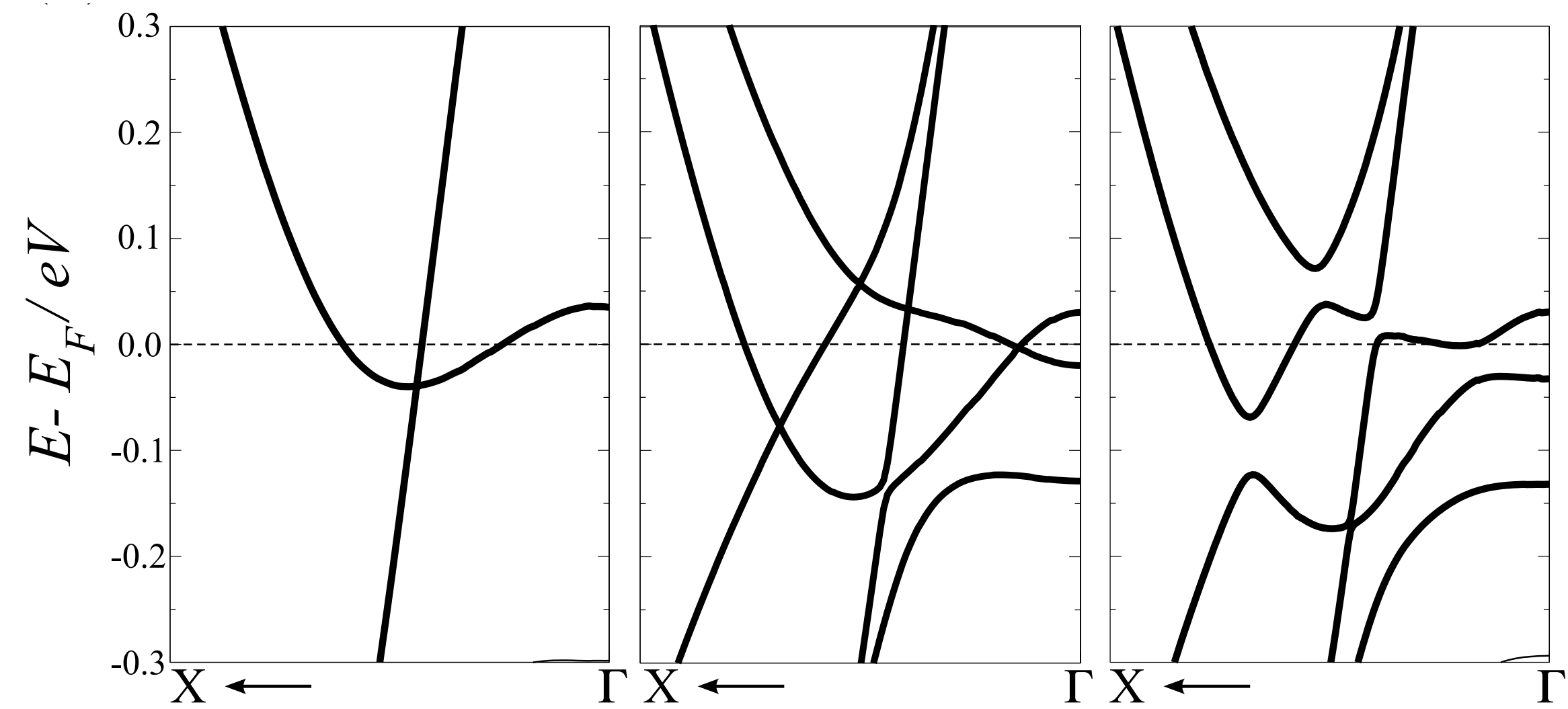
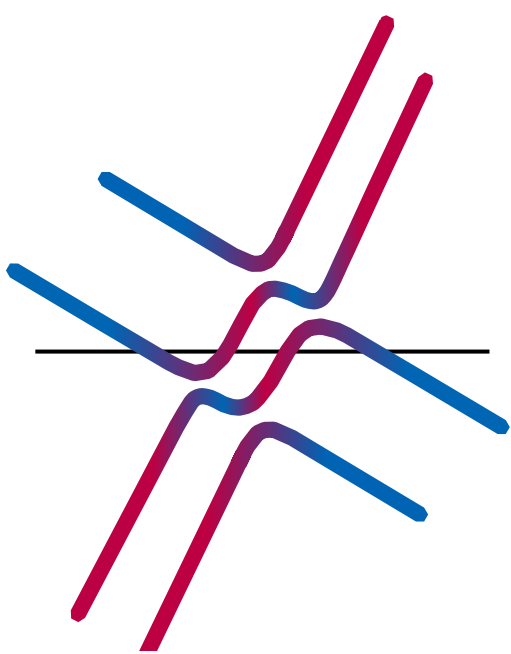
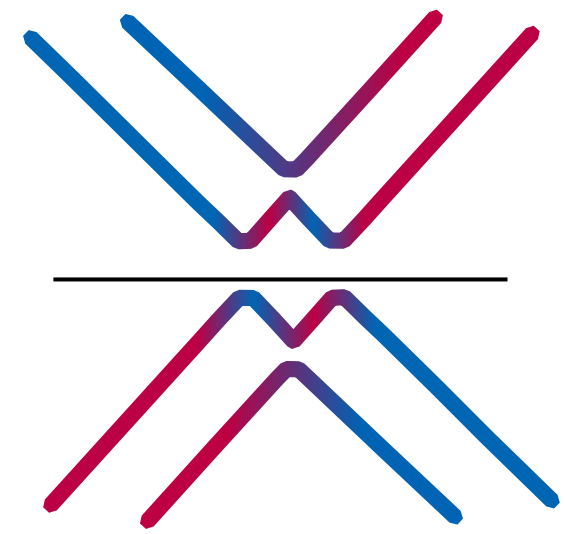
*monolayer with screw symmetry*



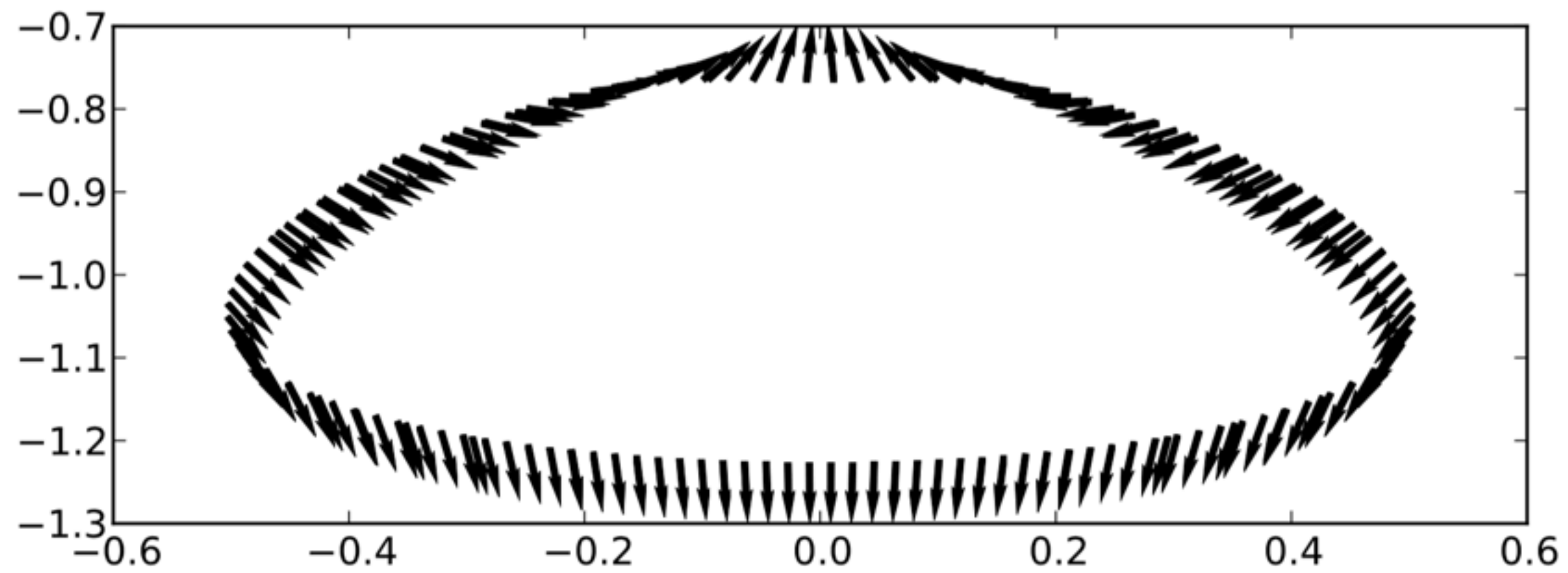
*weakly coupled bilayer with screw preserving hybridization terms*



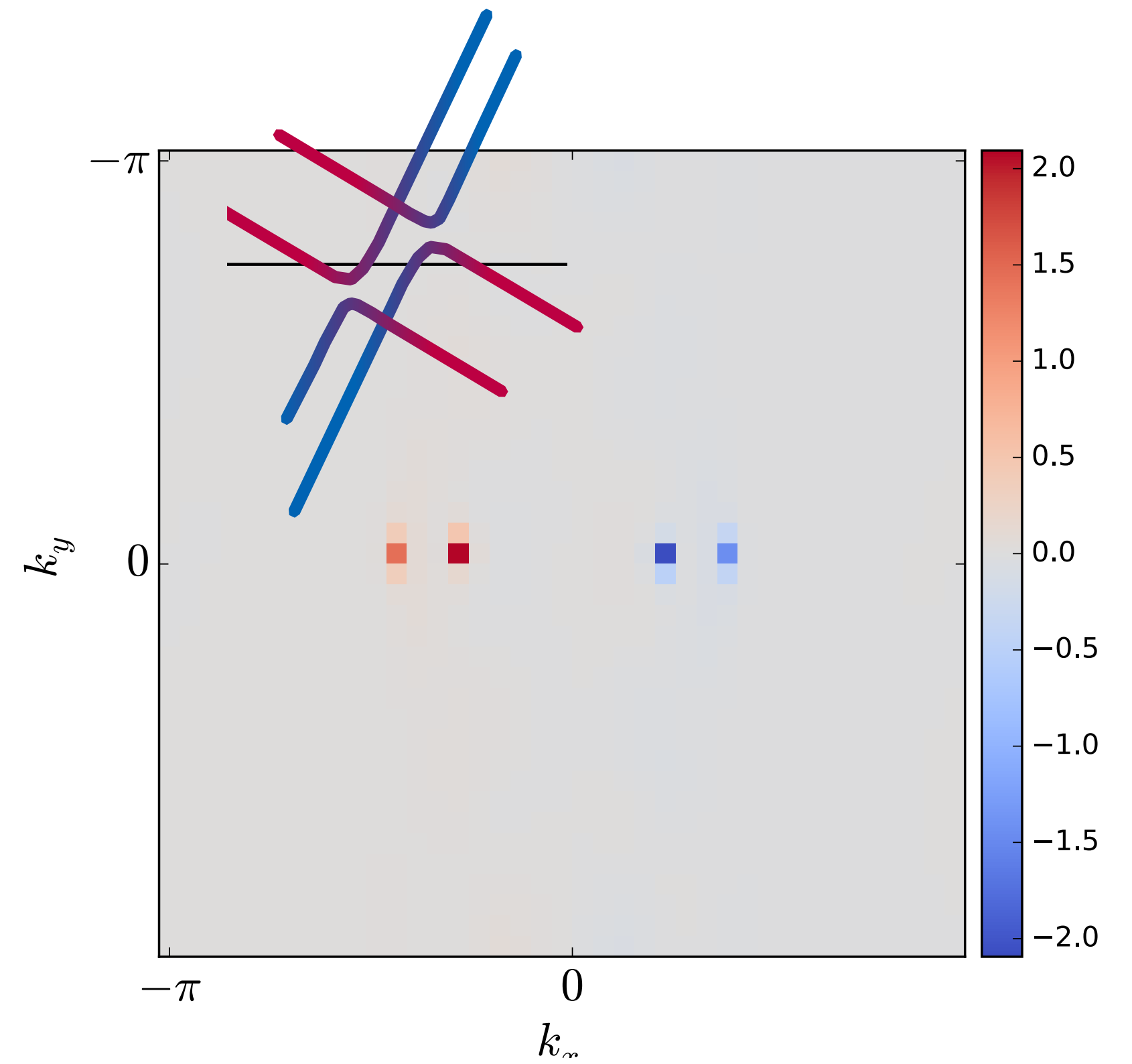
*weakly coupled bilayer with screw breaking hybridization terms*



# Consequences: transport



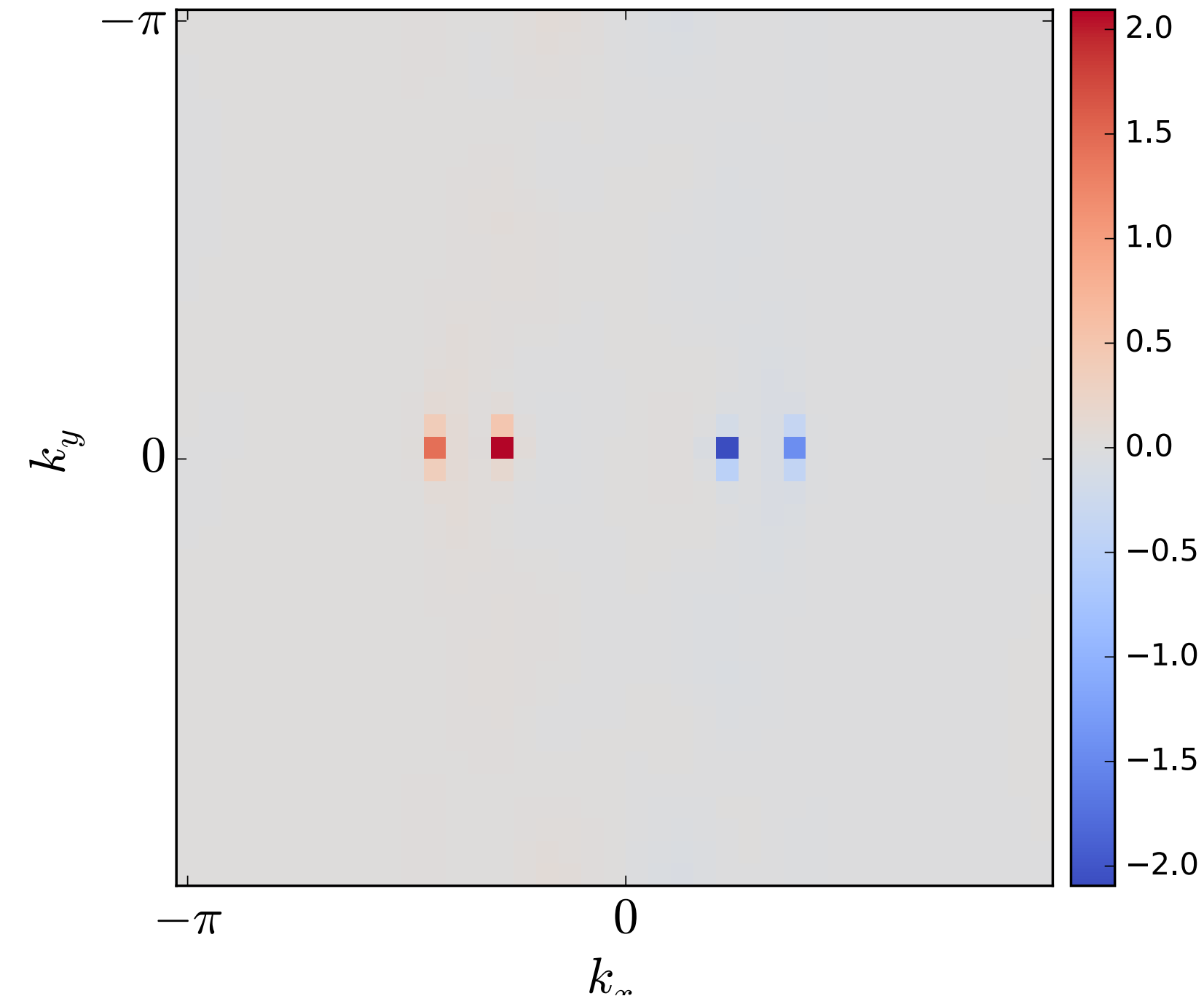
Pseudospin winding in monolayer



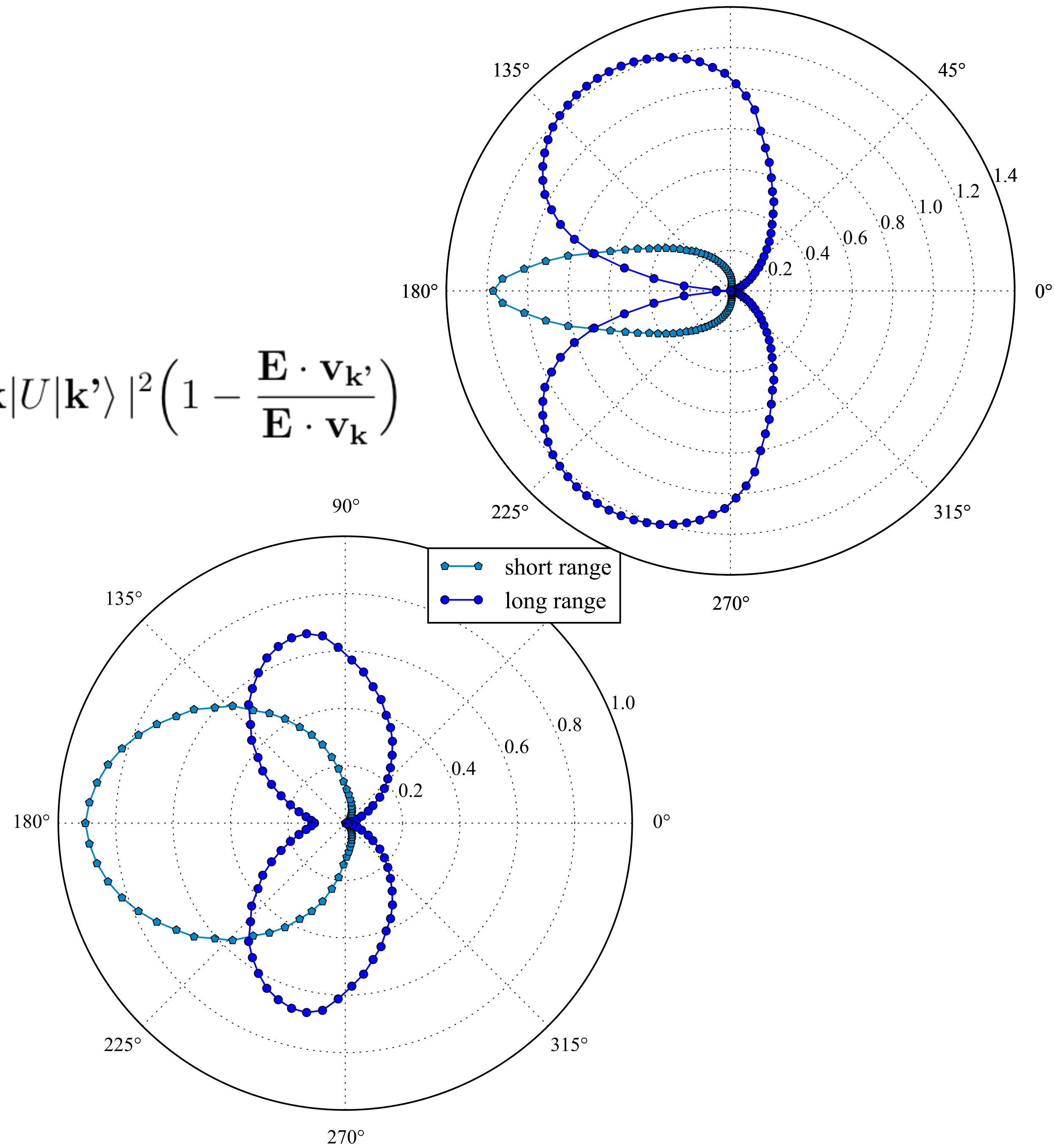
Berry curvature around electron and hole pockets in bilayer  $\text{WTe}_2$

# Consequences: transport

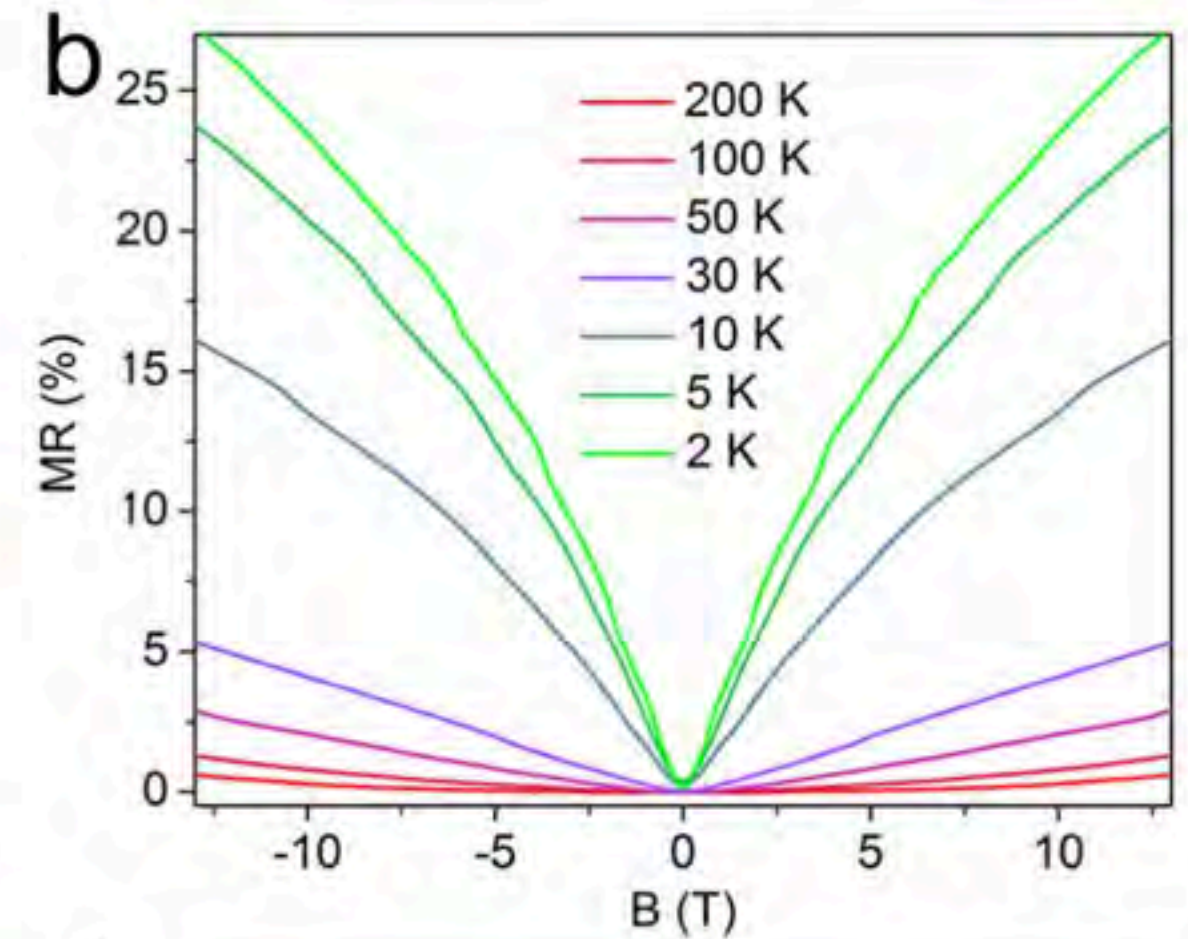
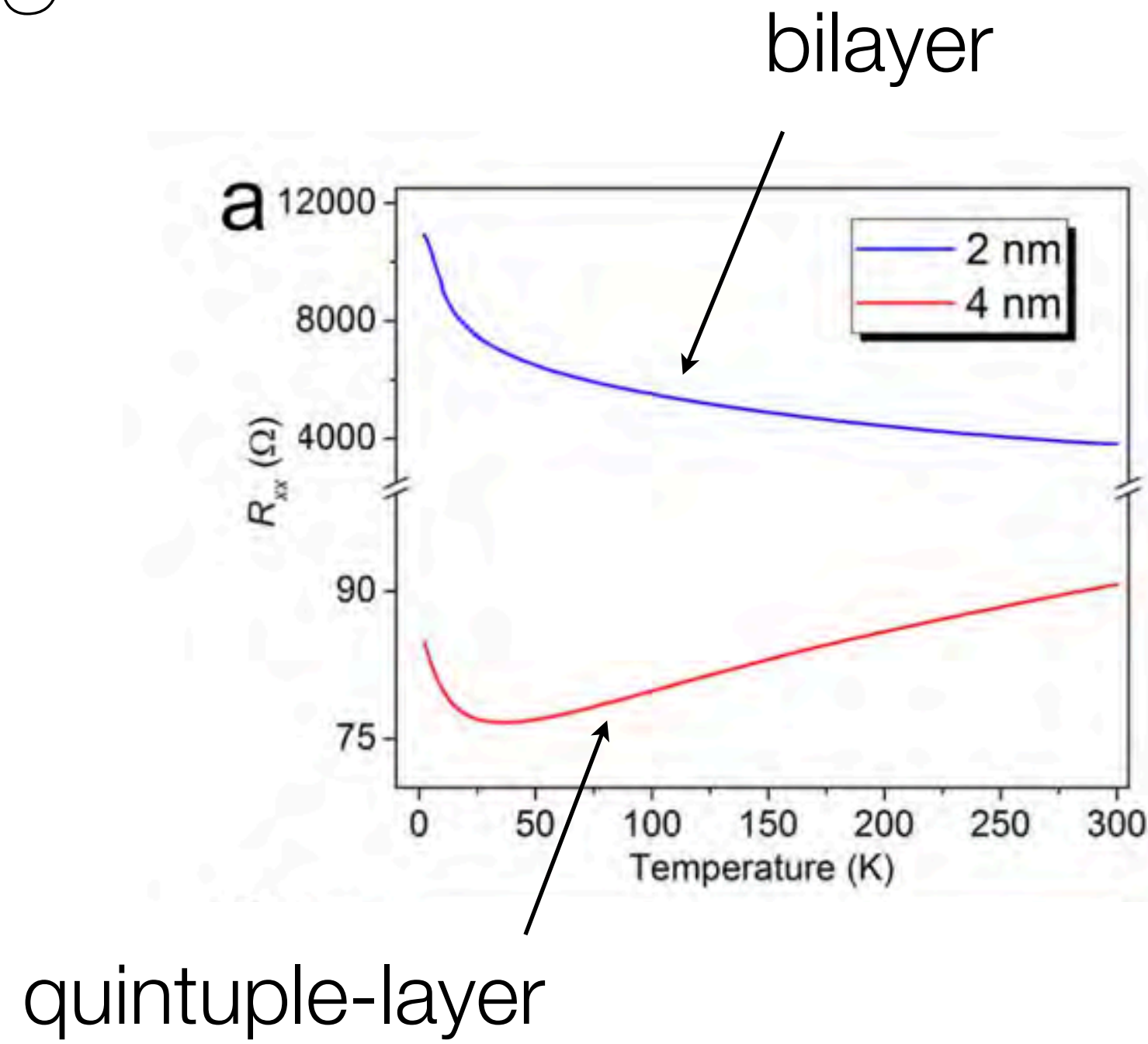
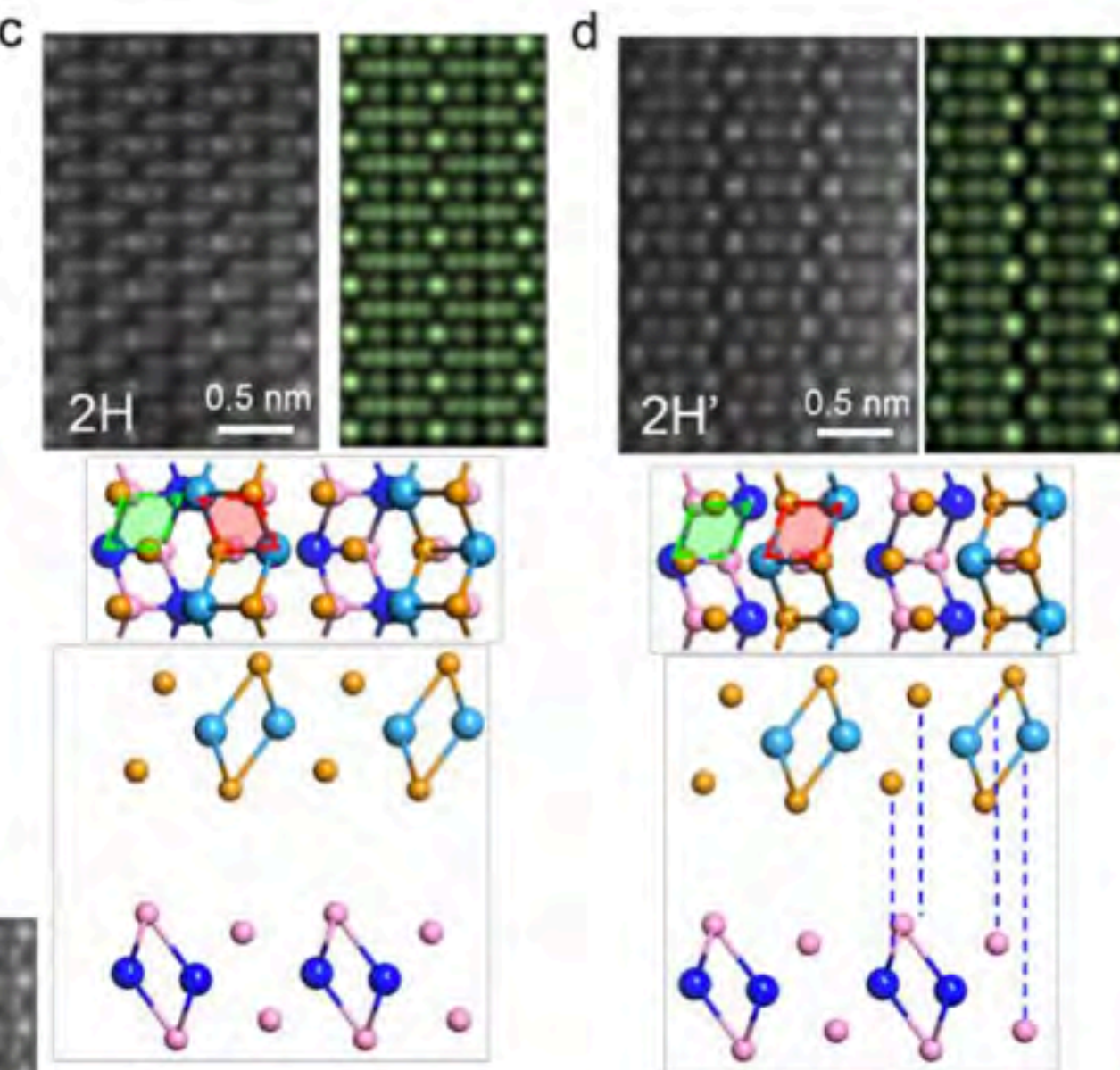
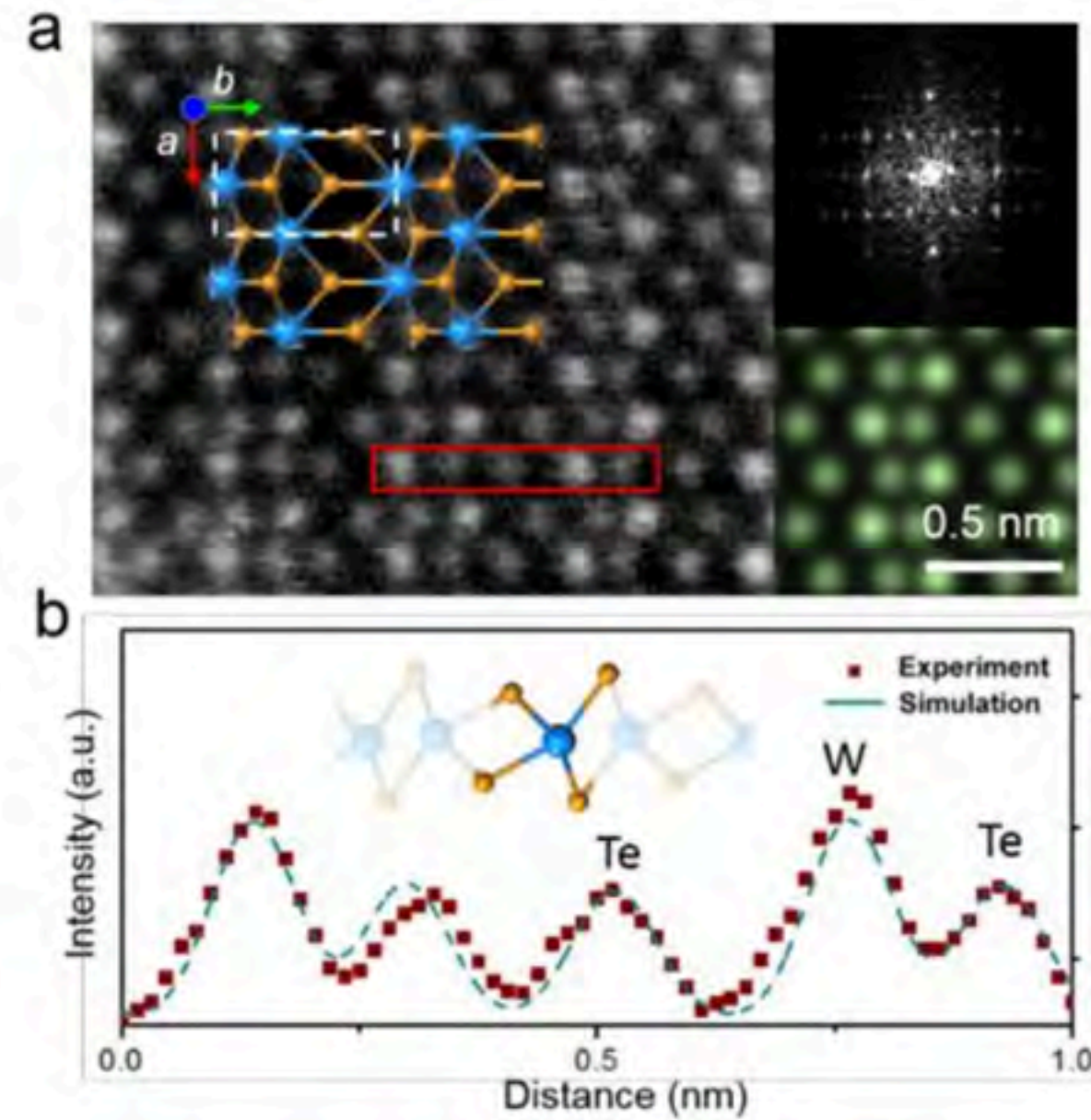
Berry curvature around electron and hole pockets in bilayer  $\text{WTe}_2$



$$\langle \mathbf{k} | U | \mathbf{k}' \rangle|^2 \left( 1 - \frac{\mathbf{E} \cdot \mathbf{v}_{\mathbf{k}'}}{\mathbf{E} \cdot \mathbf{v}_{\mathbf{k}}} \right)$$



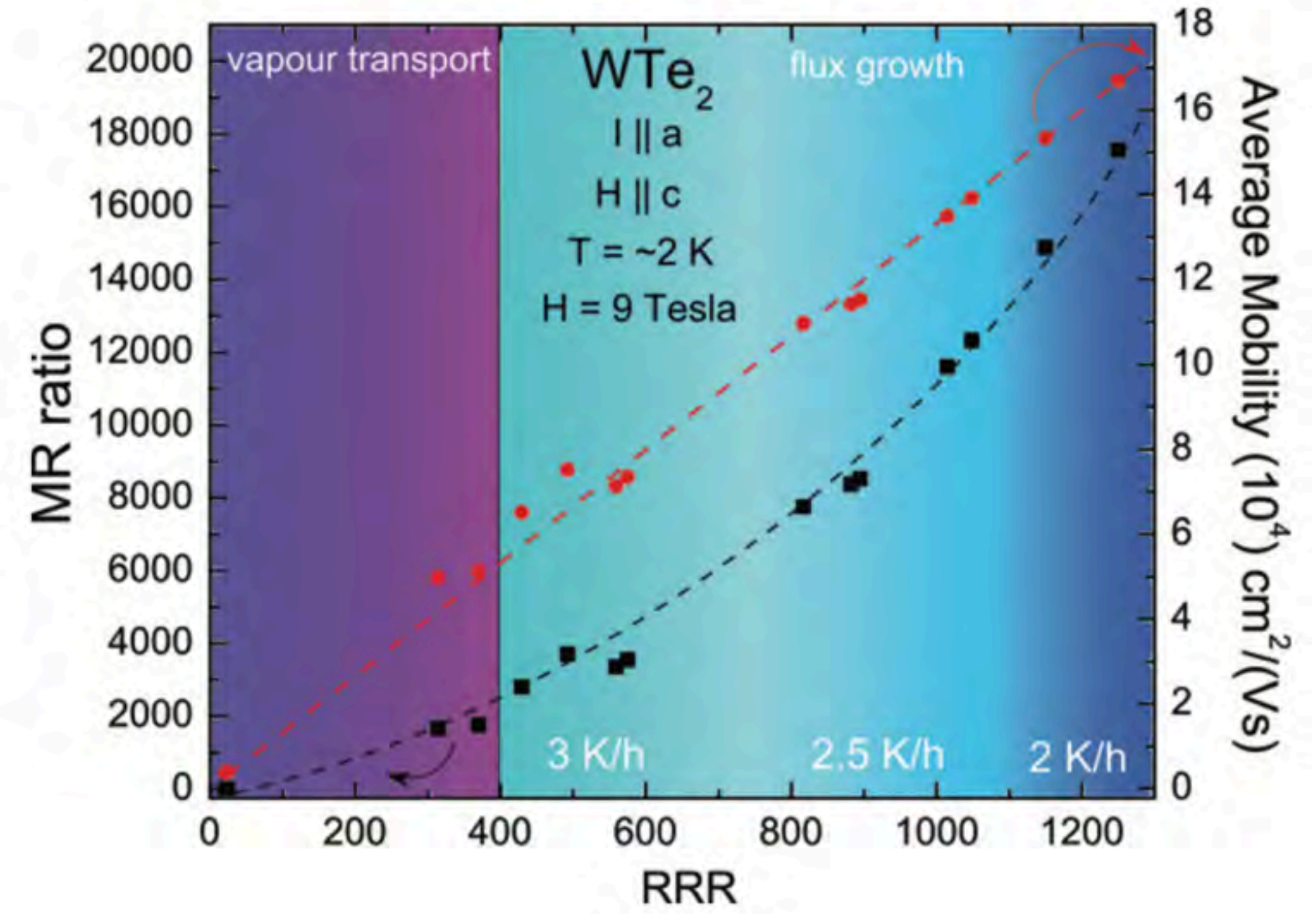
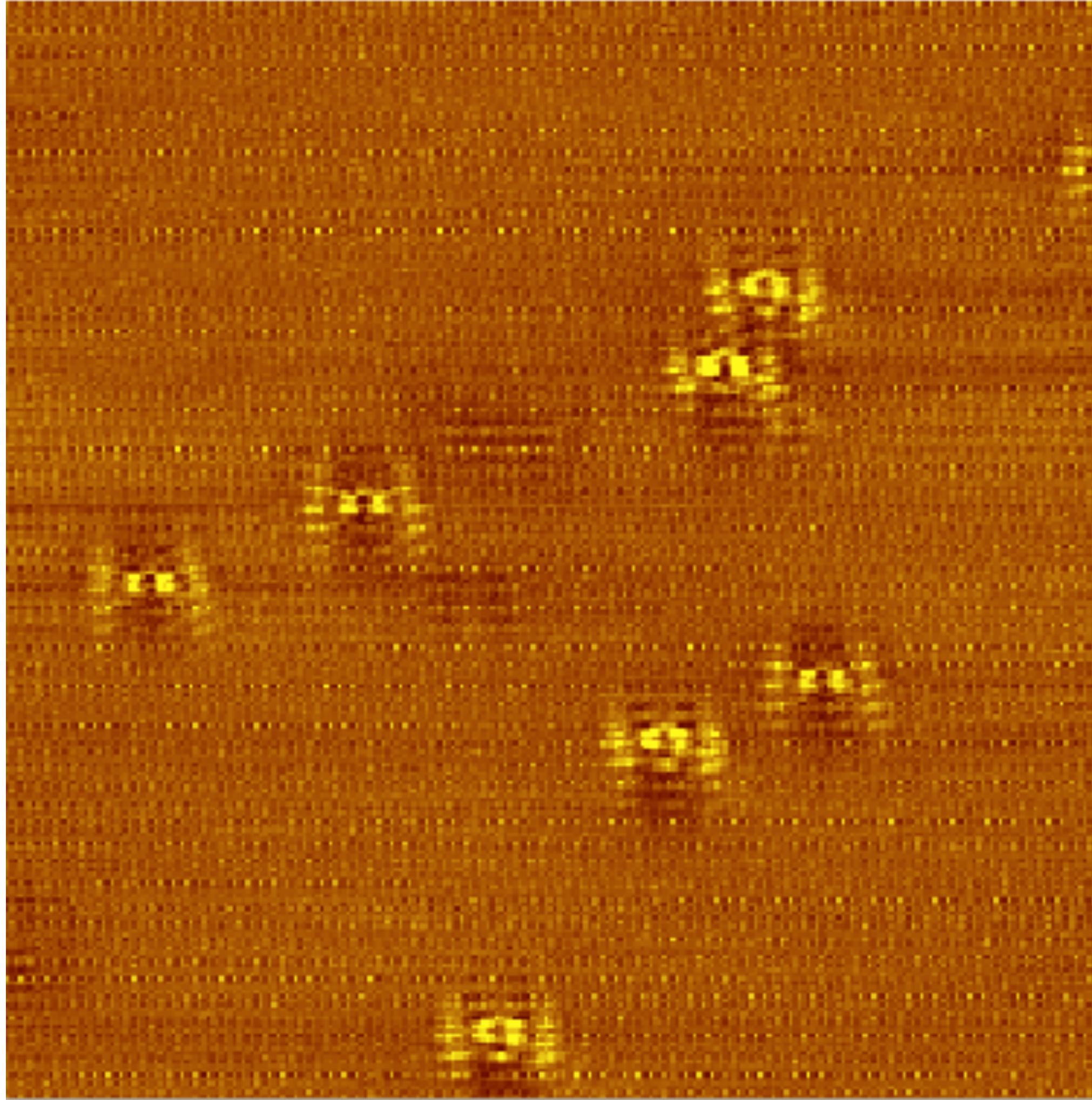
# Experimental evidence



in Fig. 4b. These results show that large and non-saturating magnetoresistance is preserved in our CVD-grown  $\text{WTe}_2$  even down to a bilayer sample, which further demonstrates their high quality. The MR reaches a maximum value of 28% at 2 K. For the thick  $\text{WTe}_2$  flakes (12 nm), the MR is about 2000% at 25K in a field of 10T, which is shown in Supplementary Fig. S16. These values



# Experimental evidence



30 x 30 nm (Yazdani group)

# Circular Dichroism

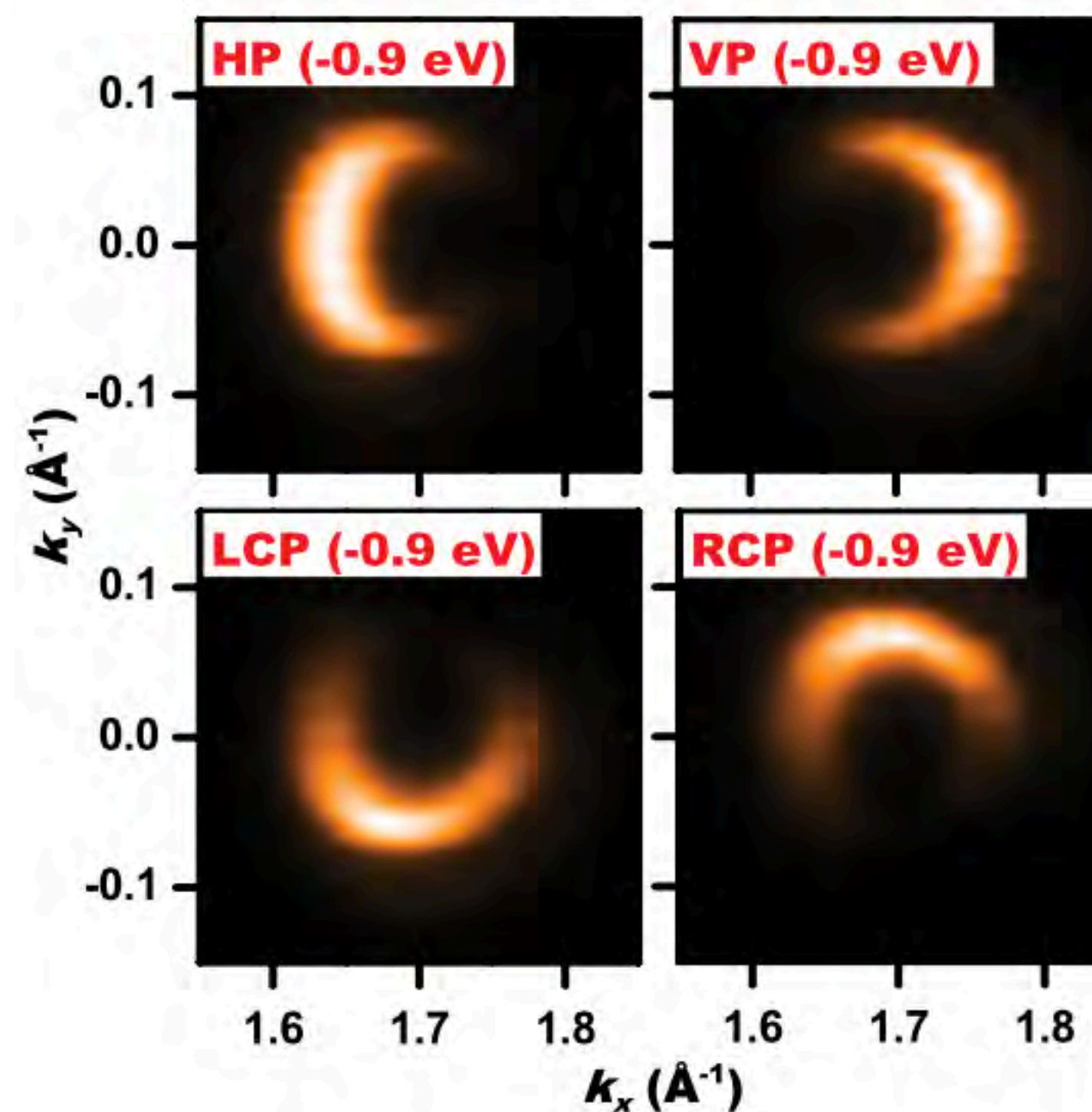
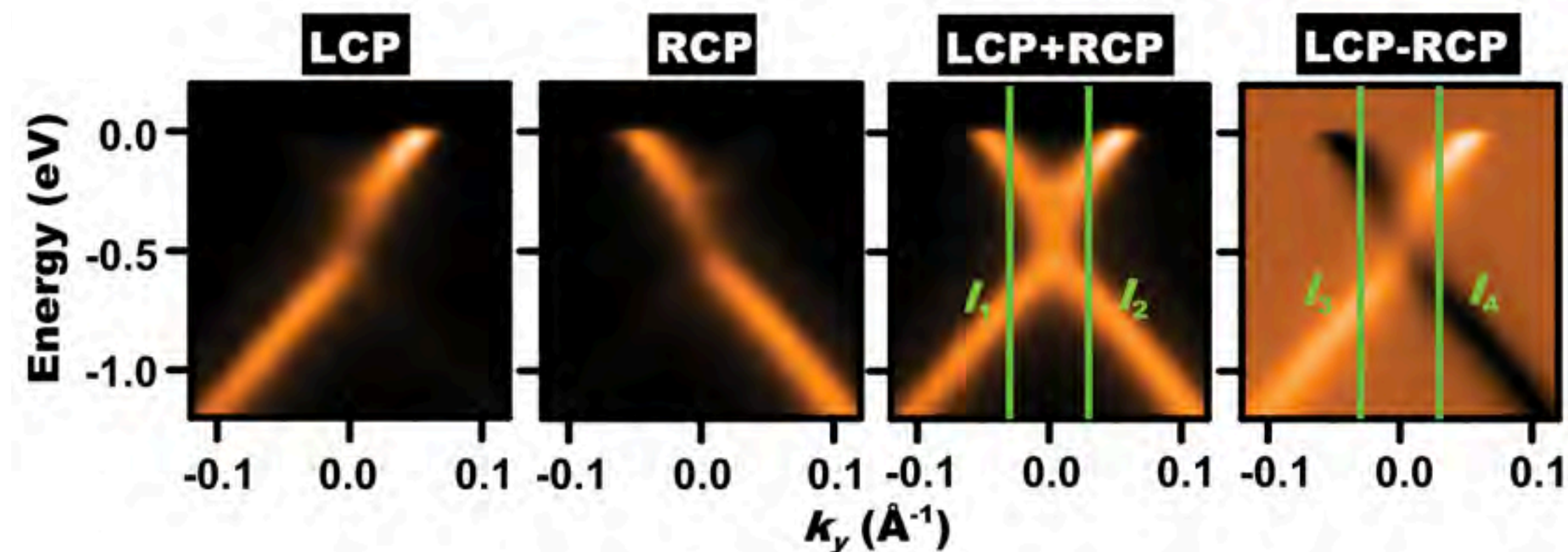
- ▶ phase sensitive tool to probe electronic structure
- ▶ Can capture effects of Berry's Phase

▶  $I_{\lambda}(\mathbf{k}, E_{\text{kin}}, \hbar\omega)$

$$\propto \sum_{i,f} |P_{\lambda}^{if}(\mathbf{k})|^2 \delta(E_f - E_i - \hbar\omega) \delta(E_{\text{kin}} - [E_f - \phi])$$

▶  $P_{\pm}^{if}(\mathbf{k}) = \lambda_{\pm} \cdot \langle f, \mathbf{k} | \mathbf{p} | i, \mathbf{k} \rangle$

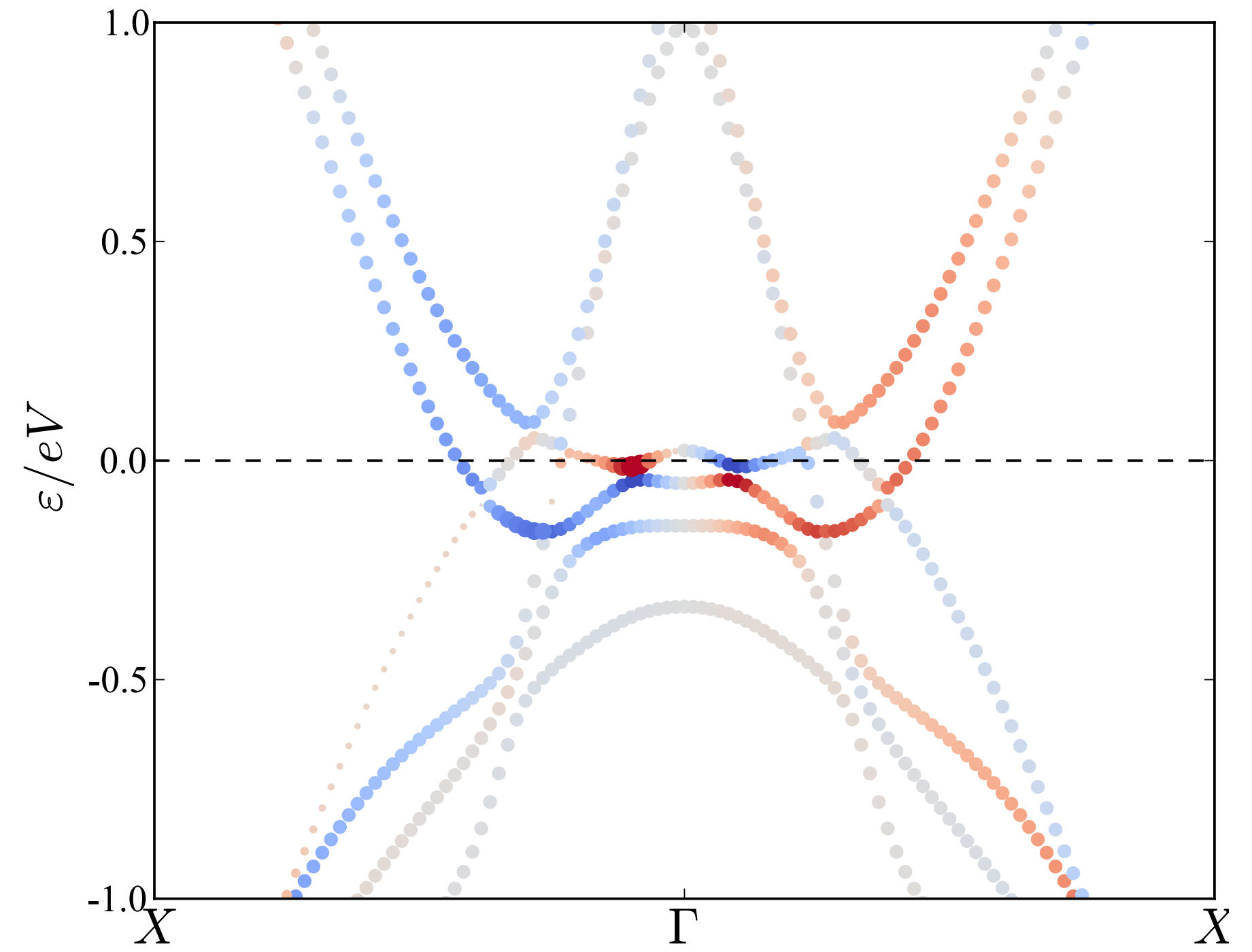
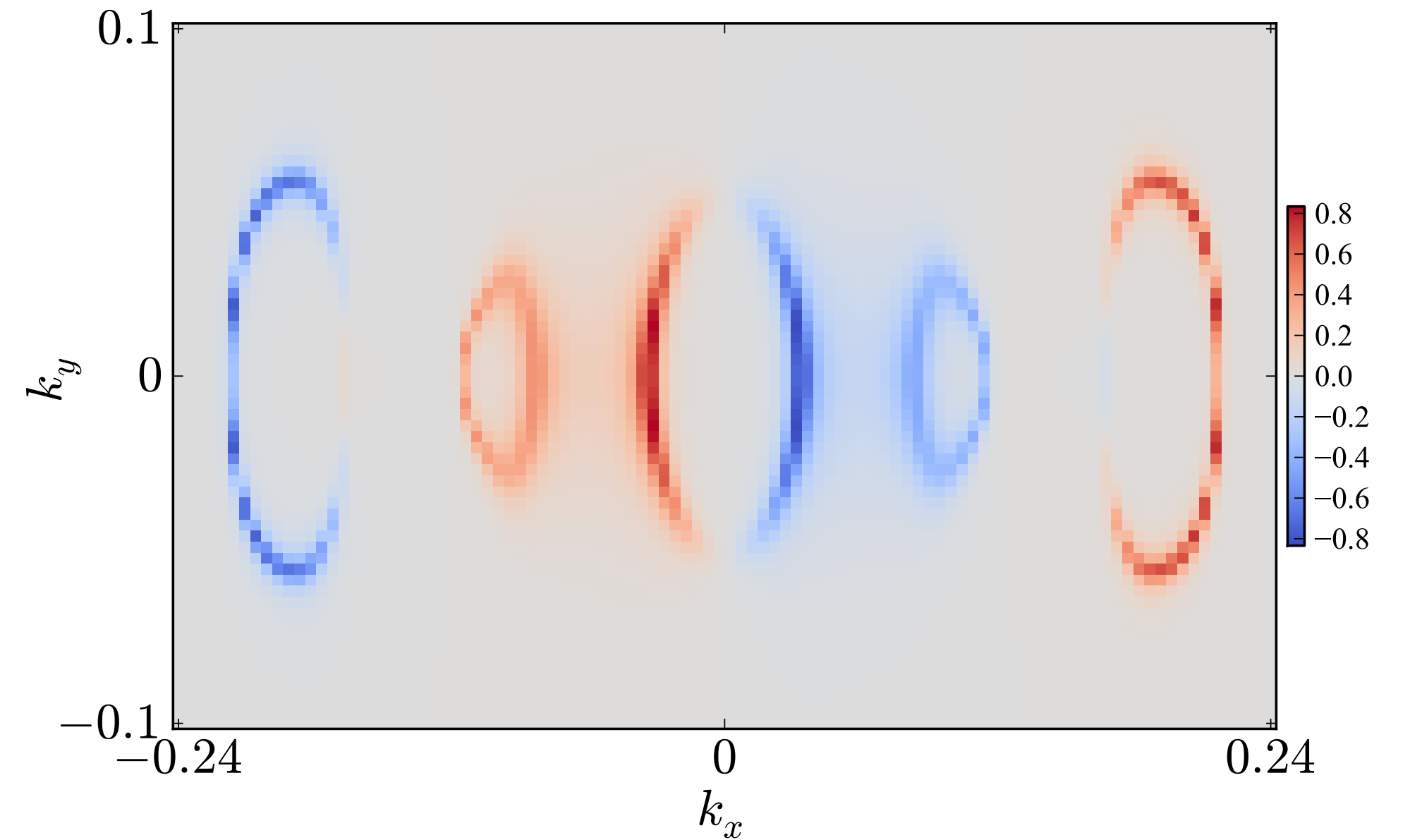
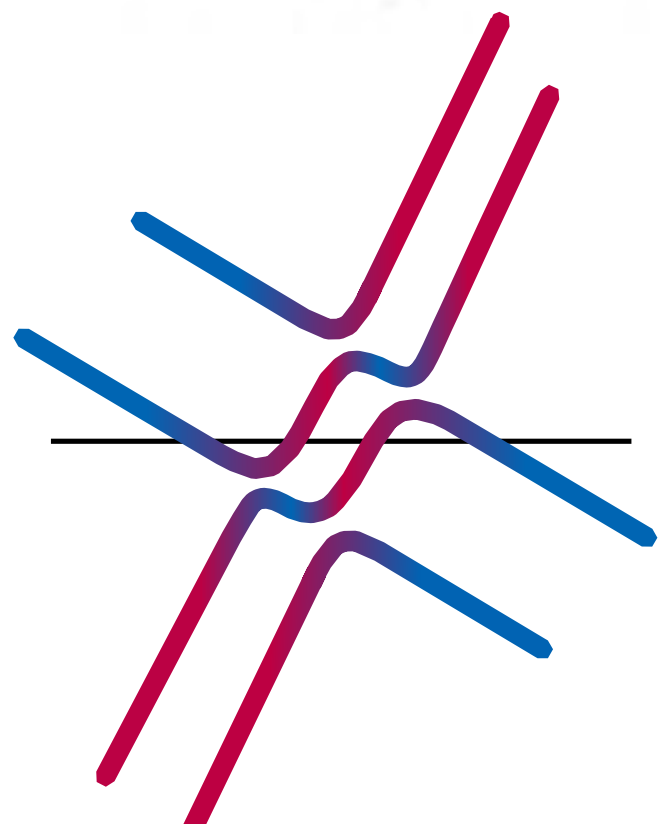
▶  $D_s(\mathbf{k}) := I_+(\mathbf{k}, E_f) - I_-(\mathbf{k}, E_f)$



# Circular Dichroism

- ▶ use of ab-initio wavefunctions for initial states at Fermi level
- ▶ Final state is totally symmetric combination of plane waves with longest wavelengths (most simple approximation possible)

$$P_{\pm}^{if}(\mathbf{k}) = \lambda_{\pm} \cdot \sum_{\mathbf{G}} \mathbf{G} c_{\mathbf{G}\mathbf{k}}^{[f]*} c_{\mathbf{G}\mathbf{k}}^{[i]}$$

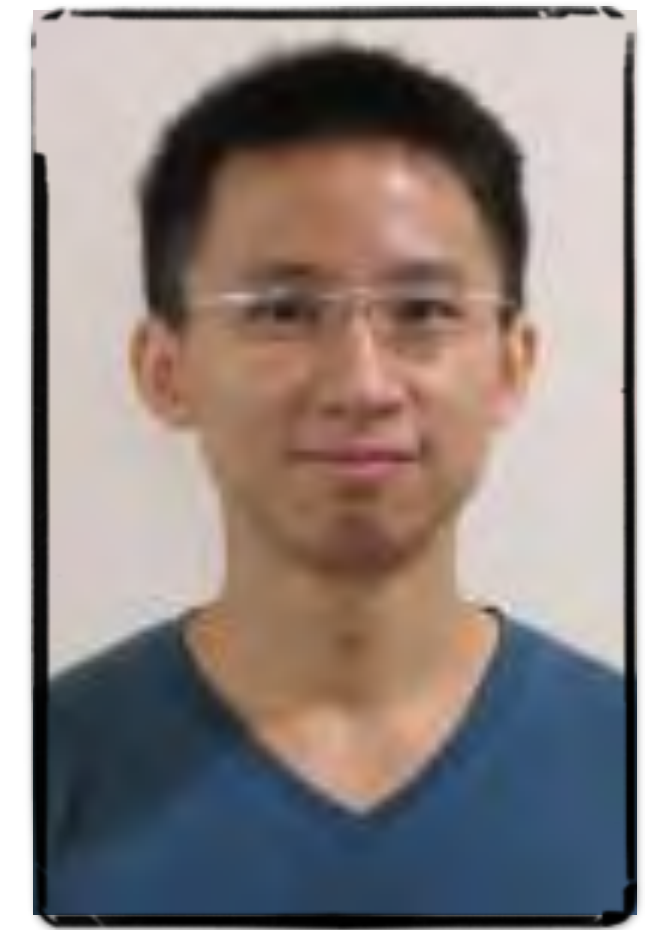


# Summary

- ▶ New topological band inverted 2D semimetal in non-symmorphic crystal structures
- ▶ Topological classification using non-abelian Wilson loops along non-contractible loops
- ▶ Monolayers  $\text{MoTe}_2/\text{WTe}_2$  without SOC as material examples
- ▶ Non-trivial monolayer structure has consequences for the 3D materials



Roberto Car



Aris Alexandradinata



Titus Neupert